2019

Adolescent Binge Alcohol Exposure Effects on Heart Structure and Function

Lizhuo Ai

LOYOLA UNIVERSITY CHICAGO

ADOLESCENT BINGE ALCOHOL EXPOSURE EFFECTS ON HEART STRUCTURE AND FUNCTION

A THESIS SUBMITTED TO

THE FACULTY OF THE GRADUATE SCHOOL

IN CANDIDACY FOR THE DEGREE OF

MASTER OF SCIENCE

PROGRAM IN PHYSIOLOGY

BY

LIZHUO AI

CHICAGO, ILLINOIS

MAY 2019

ACKNOWLEDGEMENT

I would like to express my deep gratitude to my mentor Dr. Jonathan A. Kirk for his guidance and support throughout this thesis project. I would also like to express my great appreciation to my thesis committee Dr. Seth L. Robia and Dr. Toni R. Pak for their valuable and constructive suggestions on this project. I would like to acknowledge various people for their contribution to this project: Ms. Edith Perez, for her assistance with RNAseq sample preparation and titin gel modification; Dr. Quan Cao, for echo measurements on the rats; Dr. AnnaDorothea Asimes, for teaching me the background information about the adolescent binge alcohol exposure rat model; Dr. Andrei Zlobin, for his help with RNAseq data analysis; and Dr. Chaitanya Gavini, for his assistance on plasma triglyceride and cholesterol assays; Dr. Mary Papadaki, for her help with teaching me heart dissections.

Finally, I would like to thank my parents for their support and encouragement throughout my master program.

TABLE OF CONTENTS

LIST OF TABLES

LIST OF FIGURES

CHAPTER ONE

OVERVIEW AND HYPOTHESIS

Approximately 1 in 6 adolescents report regular binge alcohol consumption, based on the National Institute of Alcohol Abuse and Alcoholism. Binge alcohol consumption is a pattern of drinking that elevates blood alcohol content to 0.08 g/dL within 2 hours. Adolescent binge alcohol exposure hampers normal brain development [1]. However, the effects of adolescent binge alcohol consumption on the heart are almost entirely unknown. Many studies have shown that alcohol consumption leads to complications such as cardiovascular dysfunction, inhibition of myocardial fatty acid metabolism, and ventricular hypertrophy and dilation, which can all lead to alcoholic cardiomyopathy in adults [2-4]. The body grows rapidly during adolescence, and in order to meet the increased oxygen demand and functional working tasks, the heart grows concurrently to increase cardiac output [5, 6]. Yet, little is known about how binge alcohol exposure impacts the growing heart.

Heart function and growth are supported by fatty acid metabolism, the preferred energy utilization of the heart [7]. However, alcohol interrupts heart fatty acid metabolism, and some key fatty acid metabolic genes have been shown to be down-regulated in hypertrophied hearts [3][8], which suggests that adolescent myocardial fatty acid metabolism may also be altered by binge alcohol exposure. In addition, alcohol consumption induces cardiac remodeling [9], and it is well studied that β-adrenergic

signaling regulates normal heart function [10] as well as remodeling during heart failure in adults [11, 12]. One possibility is that alcohol exposure alters the heart structure by directly stimulating β-adrenergic activation. We hypothesize that binge alcohol exposure negatively impacts cardiac growth, activates β-adrenergic signaling, and decreases fatty acid metabolic gene expression in the heart during adolescence.

We will address this hypothesis in the following two aims:

Aim 1: Assess cardiac structural and functional changes from binge alcohol exposure during adolescence. One critical question is whether binge alcohol consumption interrupts heart development in adolescence. It is my working hypothesis that upon binge alcohol exposure, adolescent rats will have impaired cardiac function and increased cardiomyocyte hypertrophy. We will adopt an established outbred adolescent male rat model to analyze how binge alcohol exposure affects the heart structure and function from postnatal day (PND) 36 to 44 (12-17 years in human). We will perform echocardiography (M-mode and Doppler) at both baseline and post treatment to assess cardiac structure and function. Immediately after sacrifice, blood alcohol content will be measured to ensure the binge level of alcohol exposure. Plasma corticosterone level will also be measured to control for the effect of alcohol stress on heart remodeling. Histological staining will be used to determine individual cardiomyocyte hypertrophy.

Aim 2: Determine the changes on β-adrenergic signaling and fatty acid metabolic genes in the heart after adolescent binge alcohol exposure. Changes to β-adrenergic signaling and metabolic substrate utilization are common indications of stress responses in the heart. It is my working hypothesis that binge alcohol exposure increases β-adrenergic signaling as a short-term compensatory mechanism and decreases the fatty

acid metabolism gene expressions in the heart. We will identify whether binge alcohol exposure activates β-adrenergic signaling by PKA activity assay and western blot of downstream protein phosphorylation. We will use LV tissue for RNAseq and RT-qPCR to test the expression of overall gene expression changes in those rats, including several key metabolic genes that regulate the fatty acid metabolism pathway. The plasma lipid profile, as well as LV tissue triglyceride content, will be tested to determine possible alteration on fatty acid metabolism to the body and specifically the heart by binge alcohol exposure.

Adolescent binge alcohol consumption has become a growing problem worldwide. This project allows us to improve our knowledge on how binge alcohol consumption affects cardiac structure and function in the growing heart.

CHAPTER TWO

LITERATURE REVIEW

Binge Alcohol Consumption among Adolescents

Alcohol is the most commonly used and abused drug among youth in the United States, based on statistics from the Centers For Disease Control and Prevention. The 2015 National Survey on Drug Use and Health (NSDUH) showed 33.1% of the survey population have had at least 1 alcoholic drink by 15 years of age [13]. Adolescents aged 12 to 20 years drink 11% of all alcohol consumed nationwide, and more than 90% of alcohol is consumed in a heavy episodic (binge) pattern [14]. Binge alcohol consumption is a pattern of drinking that elevates blood alcohol content to 0.08 g/dL within 2 hours. Alcohol has many negative psychological and pathophysiological consequences in adolescents. Teenagers who start consuming alcohol before age of 15 are 4 times more likely to be alcohol-dependent later in their life [15, 16]. Heavy alcohol consumption increases risks of early death such as car crashes and suicides [17]. For pathophysiological changes, alcohol can permeate to virtually all tissues in the body, which can lead to significant alterations in organ function [18]. Adolescent alcohol misuse is associated with increased neurobiological changes, and an increased risk of developing alcohol usage disorder (AUD) later in adulthood [19]. Brain development, especially the hypothalamus, has shown to be particularly vulnerable to binge alcohol

exposure in adolescence [1, 20]. However, the effects on the heart from adolescent binge alcohol consumption are poorly understood.

Normal Cardiac Growth during Adolescence

Adolescence is a period of rapid growth for both the body and the heart. The heart grows concurrently along with the increase in body weight [21]. Cardiomyocytes, the heart muscle cells, are the contracting cells and contain basic contractile units called sarcomeres, which are arranged in both series and parallel with each other. Cardiomyocytes become terminally differentiated shortly after birth and mostly lose the ability to proliferate, although a very low level of cardiomyocytes may maintain proliferative ability [22, 23]. In order to maintain metabolic demands, heart growth during childhood and adolescence is by a process called physiological hypertrophy [23]. Hypertrophy itself is defined as increased ventricular volume with coordinated growth in wall thickness, where individual cardiomyocytes increase size in both length (eccentric) and width (concentric) [23]. During physiological hypertrophy in childhood and adolescence, cardiomyocytes become bi-nucleated or multi-nucleated and the cardiac function is increased or preserved [23]. Adolescent heart growth is regulated by hormones such as growth hormone [24], insulin-like growth factor 1 [25], as well as thyroid hormones [22]. By the end of adolescence (20 years old), postnatal hypertrophy can increase heart mass by two-fold or greater due to the increase in dimensions of cardiomyocytes [23, 26].

Beta-Adrenergic Signaling Activation in the Healthy Heart

Healthy heart function is constantly regulated by the sympathetic nervous system. The function of sympathetic signaling is to trigger the body's "fight or flight response" in order to increase cardiac performance. Two kinds of catecholamines (CAs):

Norepinephrine (NE, produced primarily in sympathetic nerve endings and to a lesser extent in the adrenal medulla), and Epinephrine (Epi, produced in the adrenal medulla), are released to the circulation to act on the beta-adrenergic receptors in organs and tissues including the heart [10]. CAs bind to the beta-adrenergic receptors (βARs) on the cardiomyocyte surface, which then activates stimulatory G proteins (Gs). Gs protein stimulates the effector adenylate cyclase (AC), which converts adenosine triphosphate (ATP) to the cyclic adenosine monophosphate (cAMP) [27]. The increased cAMP binds onto protein kinase A (PKA). PKA can phosphorylate and activate multiple downstream proteins, including phospholamban (PLB) and cardiac Troponin I (TnI) [28]. Phosphorylation of PLN relieves the inhibition on the Ca^{2+}-dependent cardiac sarcoplasmic reticulum Ca^{2+} ATPase function [29]. Phosphorylation of TnI reduces myofilament sensitivity to Ca^{2+}, and therefore increases relaxation of the myofilament for the next contraction [10, 27, 28]. Beta-adrenergic pathway activation accelerates heart rate (HR), increases cardiac relaxation, and increases cardiac contractility (Figure 1) [10]. βARs are G protein-coupled receptors and contain three subtypes: β_1-ARs, β_2-ARs, and β_3-ARs. In healthy human hearts, β_1-ARs are the dominant ARs that are expressed in cardiomyocytes [30].

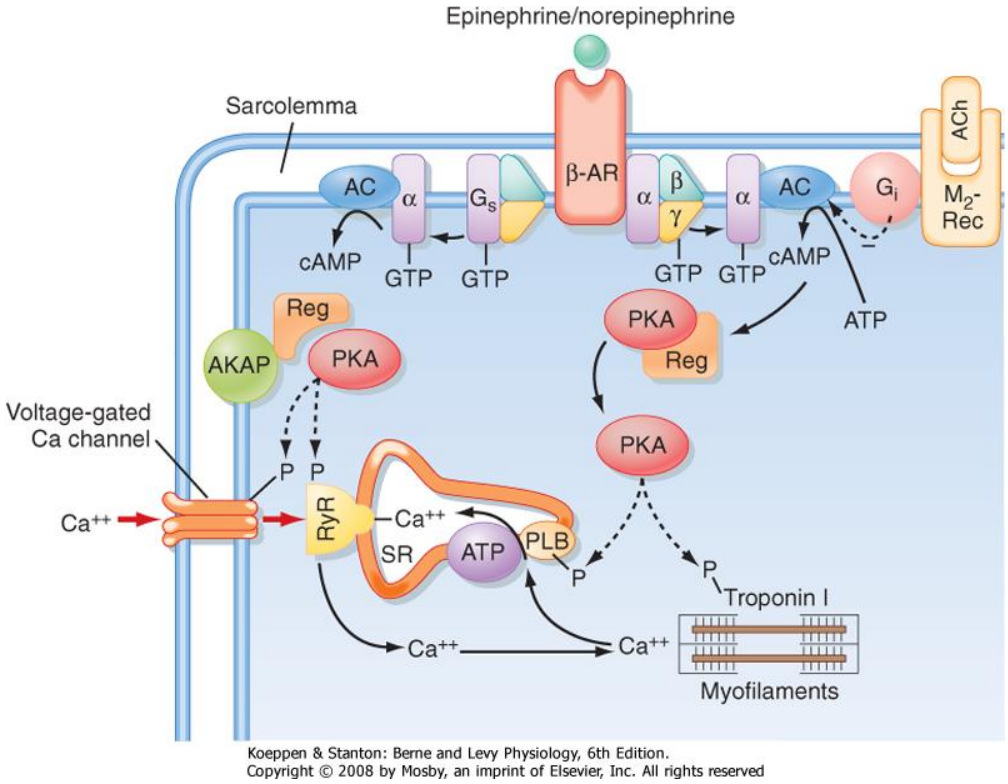

Figure 1. Schematic of Beta-Adrenergic Activation Pathway. Adapted from Berne and Levy Physiology Chapter 13 (2008). Sympathetic stimulation of the heart results in an increase in cytosolic cAMP and hence phosphorylation of several proteins by protein kinase A (PKA). An A kinase adapter protein (AKAP) adjacent to the L-type Ca++ channel facilitates phosphorylation of this channel and possibly nearby SR Ca++ channels (RyR). Other proteins phosphorylated by PKA include phospholamban (PLB) and troponin I. Muscarinic agonists (e.g., acetylcholine [ACh]), on the other hand, inhibit this sympathetic cascade by inhibiting the production of cAMP by adenylate cyclase (AC). β-AR, β-adrenergic receptor. (Redrawn from Bers DM: Nature 415:198, 2002.)

Healthy Heart Structure and Function

The mammalian heart is composed of 4 chambers: right atrium (RA), right ventricle (RV), left atrium (LA), and left ventricle (LV). Contraction and ejection of blood from the left ventricle is called systole, and immediately following is diastole when the left ventricle relaxes and refills blood from the left atria. Together systole and diastole complete one cardiac cycle. Blood flows passively from the atria to the ventricles as rapid filling (early ventricular filling), and further atrial contraction (late atrial filling) ejects the rest of blood to the ventricles during late ventricular diastole. The ratio of peak early LV filling (E)

velocity to peak atrial filling (A) velocity is a diagnostic indicator of diastolic function. Decreased E/A ratio can imply impaired LV relaxation, decreased LV compliance, and restrictive LV filling [31, 32]. Changes to the stiffness of the myofilament protein titin and remodeling of extracellular matrix are responsible for decreased E/A ratio in heart failure patients [33]. In a healthy developing human, the E/A ratio gradually increases up to 20 years old (1.88 ± 0.45, mean ± SD) and then starts to decrease as age increases (decrease muscle compliance) [31]. E/A is commonly measured by non-invasive Doppler echocardiography.

Systolic function can be measured with Motion mode echocardiography (m-mode echo). M-mode echo provides valuable diagnostic information such as the ejection fraction (EF) and fractional shortening (FS). EF is an important index for evaluating heart pumping function by measuring the fraction of blood ejected into circulation during each heart contraction [34]. The American Heart Association defines the EF for a healthy individual between 50%-70%, and EF<40% is considered cardiomyopathy. Reduced EF indicates systolic dysfunction that the heart is not able to pump enough oxygenated blood to the body. FS is another index for assessing LV muscle contractile efficiency by measuring the fraction of diastole dimensions that is reduced during the systole. End-diastolic volume is a prognostic index for ventricular dilation and LV remodeling [35].

Pathological Hypertrophy in Adults

Heart growth in adults can happen and normally has negative cardiovascular impacts. Pathological hypertrophy is normally induced when the heart is under various types of stress [10]. In order to maintain cardiac function and pump as much blood into the body, the cardiomyocytes tend to lengthen and cause LV dilation and wall thinning,

which temporally increase the filling volume during diastole [36]. However, although pathological hypertrophy initially maintains cardiac function, with activation of the β-adrenergic signaling, the key difference between physiological and pathological hypertrophy is that pathological hypertrophy ultimately leads to cardiomyopathies [36]. Pathological hypertrophy is associated with increased rates of myocyte death, fibrotic remodeling, and decreased systolic and diastolic function [23].

During heart failure, the heart is not able to pump enough oxygenated blood to perfuse the tissues. Sympathetic signaling starts to hyperactivate and overproduce CAs from the adrenal medulla and cardiac sympathetic nerve endings [27]. Short-term activation can compensate and restore cardiac function, but chronic hyperactivation of beta-adrenergic signaling causes further decrease in cardiac contractility by down-regulation of the β_1-ARs and desensitization of β_1-ARs to CAs [37, 38]. Chronic beta-adrenergic activation also negatively affects LV remodeling, fibrosis, and myocardial metabolism [27].

Repeated episodes of binge exposure have shown to continuously increase systolic blood pressure in adult rats through beta-adrenergic signaling activation [39]. However, there are no studies which link binge alcohol consumption and beta-adrenergic activation in adolescence.

Binge Alcohol Effects on the Heart in Adults

The relationship between alcohol intake and heart function is not completely linear. Light to moderate drinking (1-2 drinks) has shown cardioprotective effects by reducing coronary artery disease [40]. However, binge pattern alcohol consumption has always been shown to lead to deleterious cardiovascular effects in adults. Acute binge alcohol

exposure (drink excessively on a Saturday night out) can transiently increase blood pressure during the period of intoxication [41]. Binge drinking at least once per month over the course of a year in young men (18-45) increased resting systolic blood pressure (SBP) and total cholesterol level compared to same age non-binge drinkers [42]. High total cholesterol in the blood can increase the risk of heart disease and stroke.

Binge plus chronic alcohol consumption (>5 years) can lead to alcoholic cardiomyopathy (ACM) [2]. ACM is a type of dilated cardiomyopathy, which is characterized by dilated LV (increased LV dimensions during diastole), normal or slightly increased LV wall thickness, increased LV mass, and (in advanced stages) a reduced LV ejection fraction to <40% [3, 43].

Titin – Determinant of Diastolic Function

The sarcomere consists of thick (myosin) and thin (actin) filaments for generating the active force and titin filaments for passive elasticity. The elastic spring like protein titin, encoded by TTN, connects Z-disk and M-band region of the half sarcomere. The TTN gene contains 368 exons and multiple splice pathways that give rise to isoforms with different spring compositions [44]. At the level of the cardiomyocyte, titin is responsible for diastolic passive tension. The passive tension depends on the expression ratio of compliant and stiff titin isoforms and the phosphorylation of residues on titin elements [45]. When the sarcomere length increases, passive tension increases along with the extension of titin. The two cardiac isoforms expressed in adulthood have been illustrated in M. LeWinter's and H. Granzier's review paper (Figure 2). The relatively small ~3.0 MDa isoform is known as N2B titin. The N2B spring portion contains tandem Ig domains, PEVK segment (rich in proline, glutamate, valine, and lysine residues), and the N2B segment.

When the sarcomere stretches, tandem Ig segments extend first and then the PEVK segment, followed by the N2B segment which elongates last [44]. The second isoform contains an extra N2A element, and is termed N2BA titin. The N2BA isoform has a longer PEVK segment and a variable number of additional Ig domains resulting in a ~3.3-3.5 MDa size [44, 46]. The longer N2BA isoform is more compliant than the shorter N2B isoform [47]. Both isoforms of titin are co-expressed in the cardiac myocyte, and the ratio determines passive stiffness [48]. In the adult rodent LV, the N2B isoform predominates, therefore passive stiffness is high [49]. In larger mammals, the N2BA isoform expression increases. The human LV has a titin isoform expression N2BA/N2B ratio of 0.6 [44, 49], therefore human hearts are more compliant than those of rodents.

Titin isoform switches have been reported in cardiac diseases. In a study on dilated heart failure canine model, a decreased N2BA/N2B ratio was found compared to normal dogs without changes in total titin expression, and therefore the heart had much increased passive stiffness [50]. However, in human end-stage dilated cardiomyopathy patients, the average N2BA/N2B ratio was shifted from approximately 30:70 in controls to 42:58, due to increased expression of N2BA-isoforms to increase the heart compliance [33, 51]. The opposite findings on titin isoform shift are thought to be possible due to the different stages of DCM, that the ratio of N2BA/N2B decreases at early stage but eventually the ratio increases in the late-stage dilated cardiomyopathy [44].

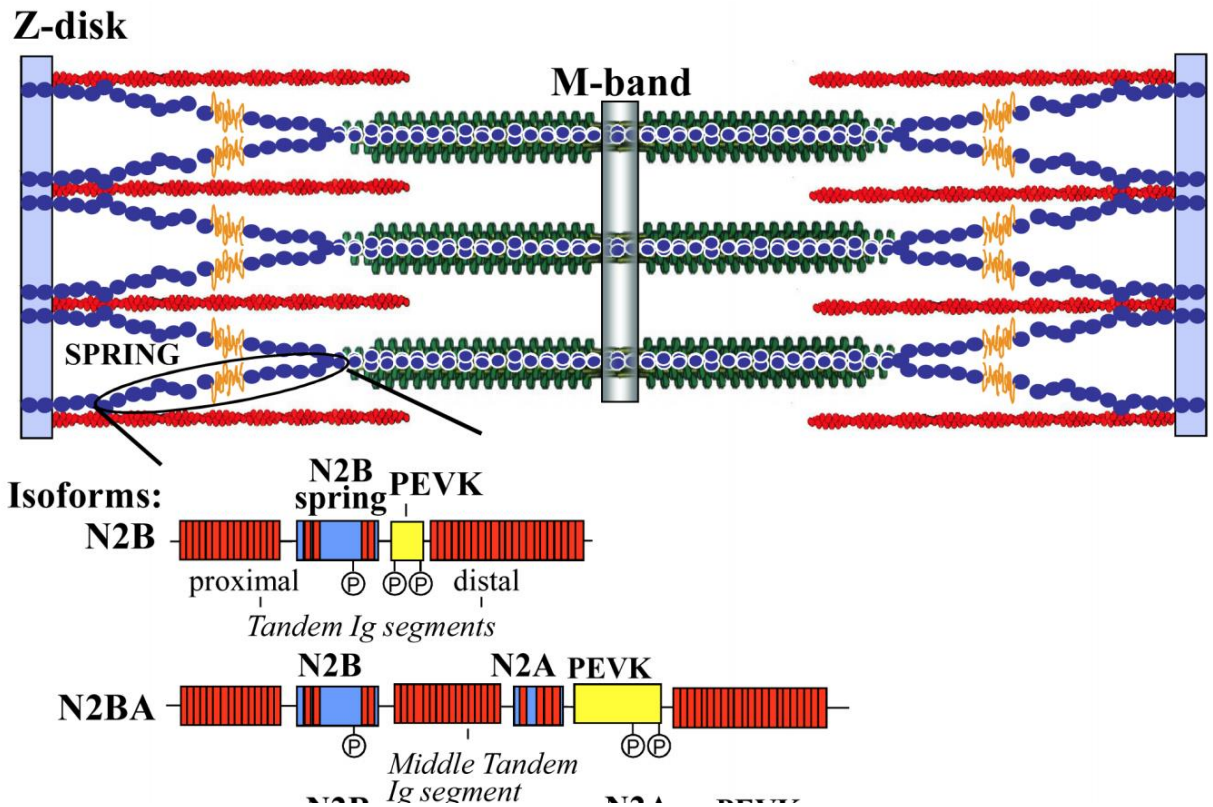

Figure 2: Schematic of Titin in the Cardiac Sarcomere. Adapted from M. LeWinter and H. Granzier (2010). N2B: shorter and stiffer titin isoform; N2BA: longer and more compliant titin isoform.

Cardiac Metabolism in the Heart

Cardiomyocytes can utilize different energy substrates such as fatty acids, carbohydrates (glucoses and lactates), ketones, and amino acids, to produce the maximum ATP for the high contractile demands. Early in cardiac development, glycolysis is the major source of energy for proliferating cardiomyocytes, and fatty acid oxidation becomes the primary metabolic pathway for generating ATP shortly after birth [23, 52]. Fatty acid metabolism provides 40%-60% of the total energy produced in the heart, with the remainder of the energy provided by glucose metabolism and other substrate metabolism [53] (Figure 3). During heart failure, cardiac energy production is normally compromised by impaired ATP production in mitochondria. Less efficient glucose

metabolism increases in the failing heart [54] and fatty acid metabolism beta-oxidation decreases [55].

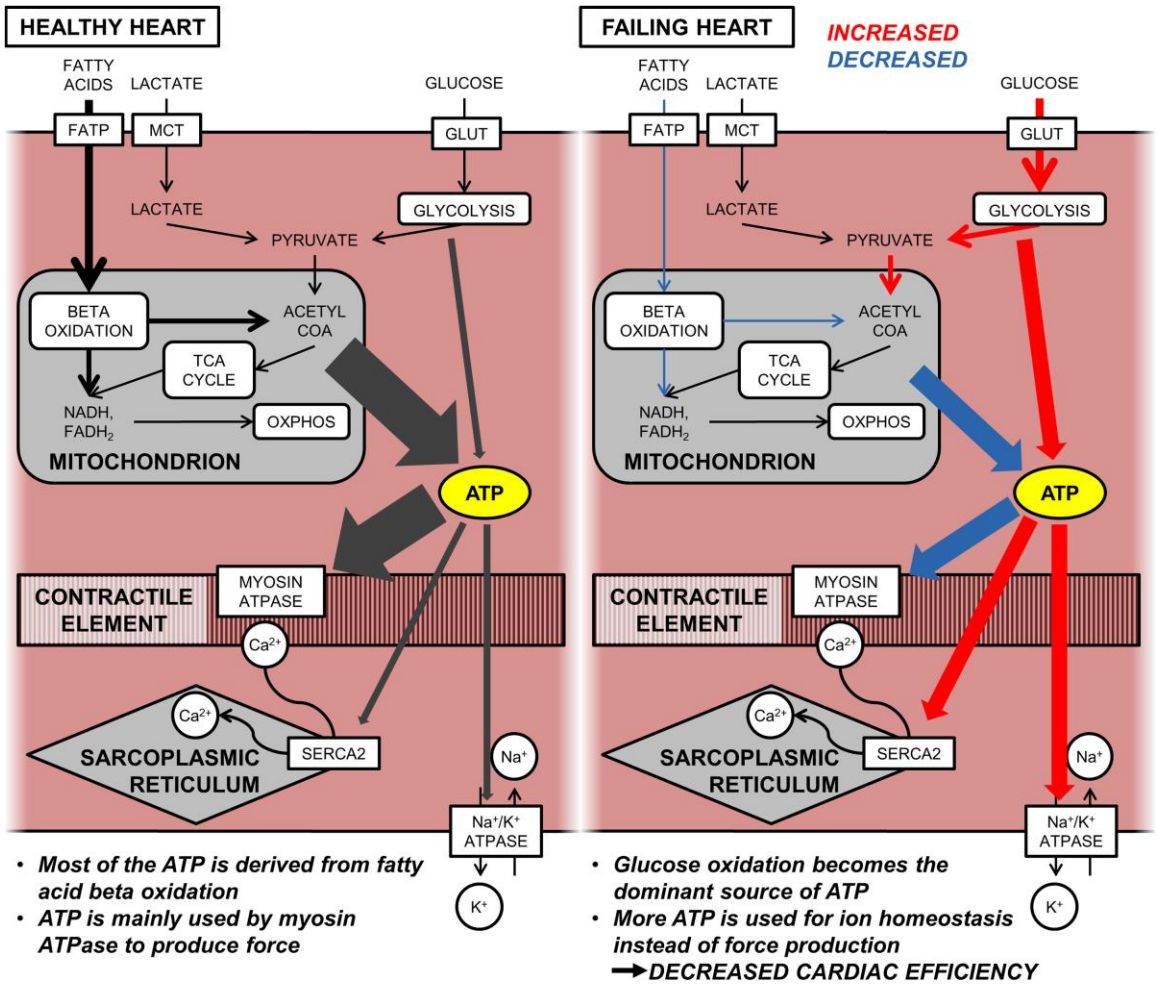

Figure 3. Energy Production and Expenditure in Cardiomyocytes of Healthy and Failing Heart. Adapted from T. Tuomainen and P. Tavi (2017). Normally, most of the cardiomyocyte ATP is produced via oxidation of fatty acids and consumed mainly by myosin ATPase in the contractile machinery to produce the force of heart contraction. In the failing heart, the metabolic phenotype shifts towards the use of glucose oxidation. At the same time, changes in ion homeostasis reduce the cardiac efficiency, which together with the impairments in energy production leads to insufficient force production. FATP, fatty acid transporter; MCT, monocarboxylate transporter; GLUT, glucose transporter; OXPHOS, oxidative phosphorylation.

Alcohol exposure is associated with changes in fatty acid metabolism gene expression. In one study, a 6 week old male C57BL/6J mouse model of chronic alcohol exposure showed increases in fatty acid uptake along with decreases in cardiac function

[56]. The protocol was for 12 weeks of chronic alcohol feeding in groups with different concentrations of EtOH (10%, 14%, 18% v/v). The treatment started when the mice were at an developmental period approximating to human adolescence to full adulthood [57]. Intra-myocardial lipid accumulation was found in all ethanol-fed groups and was significantly correlated with increased myocardial triglyceride content [3, 56]. Long-chain fatty acid uptake was evaluated in isolated cardiomyocytes and was increased in a dose-dependent manner [3, 56]. This study found Scd-1 gene up-regulation after alcohol exposure. Scd1 encodes for stearoyl-CoA desaturase 1, and it is an enzyme that catalyzes the rate-limiting step in mono-saturated fatty acid synthesis. Fatty acid synthase (fasn) and lipoprotein lipase (lpl), which are essential for de novo fatty acid synthesis, were not changed by chronic alcohol exposure in these mice [3, 56]

CHAPTER THREE

METHODS

Animals and Tissues

All animal protocols were approved by the Loyola University Chicago Institutional Animal Care and Use Committee (IACUC). Outbred Wistar male rats were purchased from Charles River Laboratory (Wilmington, MA) at the age of post-natal date (PND) 25, and they were exposed to the binge alcohol protocol between the age of PND 37 - 44, which is equivalent to the early adolescent period in human [58, 59]. When the rats arrived at PND 25, they were left un-disturbed for 5 days. Rats were randomly pair-housed within the same treatment group in environmentally controlled conditions. Rats were kept on a 12/12-hour of light/dark cycle with the lights switched on at 7 AM. Rats had free access to pellet food and water. All measures were taken to minimize pain and suffering.

At the end of the protocol, rats were euthanized by rapid decapitation immediately after echoes. Hearts were rapidly dissected out and separated by LV free wall, septum, RV, and atria immediately after euthanasia. Tissues were stored in 1.2 mL cryogenic vials (430658, Corning), flash frozen in liquid nitrogen, and stored at -80 °C. Four whole LVs from the each group (LV free wall and Septum together) were preserved differently and used for H&E staining.

Adolescent Binge Alcohol Exposure Paradigm

This thesis project utilized a well-established repeated binge alcohol exposure paradigm as previously described [1, 60] with a few small modifications as described below (Figure 4). Briefly, to minimize handling stress, each rat was pre-handled from PND 30-36 for 5 minutes at the same time from 9 AM to 10:30 AM for 7 days. On PND 30-31, we first introduced human interactions by opening the cages and had our hands leaning against each cage. On PND 32, we further interacted with the rats while they were free moving in the cage. On PND 33, we picked them up from the tail for the first time. On PND 34, we started to hold them at the scruff for several seconds in our arms. On PND 35 we introduced the gavage needles by holding the needle tip in their mouth for a few seconds. Lastly, on PND 36, we performed a dry run gavage by sending the needle down the throat to their stomach.

On PND 37, cages were randomly assigned and divided into three groups: Water, Binge, or Acute. All rats received their treatment once per day via oral gavage at the same time between 9 AM to 10:30 AM. The Binge rats were given food-grade EtOH (Everclear, 190 proof, Luxco) diluted in tap water at a dose of 3g/kg body weight (20% volume/volume) from days 1-3, water only on days 4 and 5, and back to EtOH on days 6-8. The Water group had water equivalent (3g/kg) for all 8 days. The Acute group received water equivalent for first 7 consecutive days, and EtOH for the last dose on PND 44 to account for the acute effects of alcohol present in the rat's system vs. the repeated binge pattern (Figure 4). All rats were weighed on PND 36, 38, 41, and 43 for recalculation of the gavage dose. Final body mass on PND 44 was also recorded. Water intake of each cage was measured by weighing the water bottles every other day. Food intake of each

cage was also monitored by weighing the pellet chow before and after the 8-day treatment.

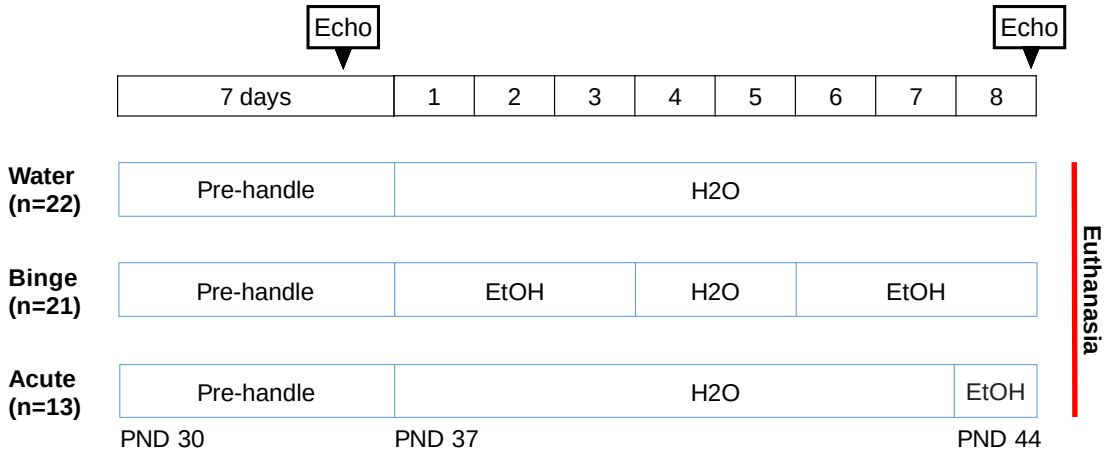

Figure 4. A 7-Day Prehandle Period Plus 8-Day Treatment Paradigm Given to Three Groups of Male Wistar Rats. All rats were given food-grade EtOH diluted in tap water at a dose of 3g/kg body weight (20% volume/volume), or water equivalent once per day via oral gavage. The Binge group received first three days and last three days of EtOH and 2 days of water gavage in between. The Acute group received water equivalent for 7 consecutive days and the EtOH for the last dose on PND 44 for control of acute alcohol stress. The Water control group received water equivalent all 8 days. Echocardiogram was performed both before the 8-day treatment and one hour within the last gavage prior to euthanasia. Baseline echo was done on PND34 during late pre-handling week, and post treatment echo was performed within the hour between the last dose of treatment and euthanasia.

M-mode and Doppler Echocardiography

Both motion mode (M-mode) and Doppler echocardiography (Vevo 2100, VisualSonics) were used to measure cardiac structure and function changes with adolescent binge alcohol exposure. Baseline echoes were performed on PND 34. Post treatment echoes were measured within one hour after the last dose of treatment on PND 44 (Figure 4). Rats were under 5% isofluorane for the initial anesthesia and then all the measurements were performed at 2% isofluorane stable state. All echo measurements were performed when rats were placed on an animal-handling platform at 37°C. Both baseline and post treatment echo measurements were performed by CVRI animal surgeon Quan Cao, MD. The LV short-axis view was used to obtain B-mode two-

dimensional images and M-mode tracings of LV posterior and anterior wall. Multiple echo measurements were captured for each rat. Heart rate (HR) was recorded while rats were under 2% stable isofluorane anesthesia.

LV end-systolic and end-diastolic diameters (LVESD and LVEDD) and posterior wall thickness at diastole (LVPWd) were measured using M-mode echo. End Diastolic Volume (LVEDV) was calculated using formula of Teichholz: LVEDV =7.0/(2.4+LVEDD) * $LVEDD^3$, and end-systolic volume was LVESV =7.0/(2.4+LVESD) * $LVESD^3$. Fractional shortening (FS), an index for systolic function, was calculated using the equation FS%=(LVEDD-LVESD/LVEDD) * 100% [34]. Stroke volume (SV) is the difference of LVEDV and LVESV of each animal, and it is the volume of blood ejected from the LV during each systolic period. Ejection fraction (EF) is the ratio of the SV to the LVEDV: EF% = (SV/LVEDV) *100%. Final cardiac output (CO), which is the volume of blood ejected from the LV to the aorta per minute, was calculated using CO= HR * SV.

Blood Alcohol Content Measurement

Blood alcohol content (BAC) measurement was performed as described previously [61]. Briefly, trunk blood from each rat was collected in heparinized tubes and centrifuged at 3,000 rpm for 10 min at 4°C. Plasma was centrifuged out and stored at -20°C. BAC was measured using Alcohol Reagent Set (A750439, Pointe Scientific, INC.) and read at 340nm absorbance using Infinite 200 PRO (Tecan). Standard curves for extrapolating the alcohol level of each rat were made based on dilutions using pre-measured alcohol standards (A7504-STD, Pointe Scientific, INC.).

H&E Histological Staining

After euthanasia, the LV free wall (n=4 in each group) was dissected out immediately and incubated in 10% formalin overnight. The tissue samples were embedded in paraffin and sent for H&E staining to the histology lab at Loyola University Chicago Medical Center. Individual cardiomyocyte concentric and eccentric hypertrophy was visualized under a light microscope (400x), and quantified by ImageJ software as previous described [2]. Image measurements were analyzed by three blinded individuals.

Corticosterone Assay

Plasma levels of corticosterone were measured using commercially available DetectX Corticosterone Enzyme Immunoassay kit (K014-H1, Arbor Assays) according to the manufacturer's instructions. Briefly, 5μL of plasma from each rat and 5μL of Dissociation reagent was pipetted into 1mL Eppendorf tubes. After vortex and incubation for 5 minutes, 490μL of diluted Assay buffer was added to achieve 1:100 dilution. Next, 50μL of the total 500μL of diluted sample was added to the 96-well plate provided from the kit. 50μL of Assay buffer was also added in each sample well. 25μL of Detex Corticosterone Conjugate as well as the same volume of Corticosternone Antibody were added separately into each sample well using a multichannel pipet. The plate was incubated at room temperature for an hour with gentle shaking. Each well was then aspirated and washed with 300μL Wash buffer 4 times. 100μL of the TMB Substrate was added into each well with a multichannel pipet and incubated for another 30 minutes without shaking. Finally, 50μL of the Stop Solution was added with a multichannel pipet. Each sample was prepared in triplicate. The plate was read at 450nm absorbance using Infinite 200 PRO (Tecan) reader to determine the optimal density (OD) of each sample.

Corticosterone level of each rat was calculated from the raw OD using 4 parameter logistic curve (4PLC) fitting.

BCA Assay

LV tissue samples were used for BCA assay (23225, Pierce ™ BCA protein Assay Kit, Thermo Fisher Scientific) to determine protein concentrations. Briefly, 2.5μL tissue homogenates from each LV sample was pipetted into a 96-well plate, and 22.5μL ddH_2O was added to achieve a final 10-time dilution. Each sample was prepared in triplicate on the plate. A ratio of 50:1 solution of Reagent A and Reagent B (provided in the kit) was prepared as the assay reagent. Then 200μL of the assay reagent was added in each well with a multichannel pipet. The plate was left on a shaker (300rpm) for 30 seconds and then transferred to a 37°C incubator for another 30 minutes. Then the plate was read at 562nm on Infinite 200 PRO (Tecan) reader. Standard curves for interpolating rat samples were made based on a series of dilutions using BSA standards provided in the kit. BCA assay was later used for equalizing sample loadings in multiple experiments: specific titin isoform gels, western blots, PKA assay, and LV tissue triglyceride level assay.

Titin Isoform Switch Gel

LV free wall tissue from each animal (30-60 mg) was kept in Standard Relaxing Buffer (SRB) solution with triton X100. Tissues were homogenized with an electric homogenizer (GLH 850, Omni International) at 7500 rpms for 3 seconds, repeated twice. After washing with SRB solution (without triton X100) and centrifuging, the pellet from each sample was weighed and solubilized in 9M urea at 1:10 (weight/volume). Samples were the sonicated for 1.5 seconds, 3 times. BCA assay was then performed to obtain the protein concentration of each sample.

We made specialized titin isoform gel using a 6% acrylamide plug (distilled water, 40% acrylamide, 0.5M Tris pH 6.8, 10% SDS, 10% APS, and 5 µL TEMED) combining with 1% agarose resolving gel. 15µg of total protein from each sample was loaded on the gel and run for 2.5 hours at 15 mA constant current at 4°C. Titin isoforms were visualized after staining with 0.2% coomassie solution overnight and fixed in de-staining solution (10% methanol and 7.5% glacial acetic acid). Additional samples were sent to Dr. Charles Chung's lab in Wayne State University for titin isoform separations.

Western Blots

Western blot samples were prepared using the same method as the titin gel preparation. Total tissue lysate (6 µg) were subjected to SDS Page using Bolt™ 4-12% Bis-Tris plus gels (NW04122BOX, Thermo Fisher Scientific) at 180 volts for 30 minutes, and transferred to nitrocellulose membrane using a wet transfer apparatus for one hour at 10 volts (1620115, Bio-Rad). The membrane was blocked with blocking buffer (Licor) in TBS and incubated with primary antibodies overnight at 4°C against cardiac phospho-Troponin I (1:1000, 4004S, Rabbit, Cell signaling) and total cardiac Troponin I (1:10,000, Mouse, IPOC Inc.). The following morning, secondary antibodies (1:10,000, Licor) were added and the membrane was then incubated at room temperature for 1 hours. Secondary antibodies were Goat anti-mouse for red channel (800nm), and Goat anti-rabbit for green channel (700nm). Membrane was visualized with Azure c600 imager (AzureBiosystems) and analyzed using Image Studio Lite software.

Plasma Triglyceride and Cholesterol Levels Measurements

Plasma levels of triglyceride and cholesterol were measured using Infinity ™ Triglycerides Reagents (TR22421, Thermo Fisher Scientific) and Infinity ™ Cholesterol

Reagents (TR13421, Thermo Fisher Scientific), according to manufacturer's instruction. Briefly, for triglyceride level, 3µL of plasma from each rat was added with 300µL Triglycerides Liquid Stable Reagent into a 96-well plate. The plate was incubated for 300 seconds at 37°C and read at 500nm using Infinite 200 PRO (Tecan) reader. For measuring cholesterol level, 3µL of plasma from each rat was added with 300µL Cholesterol Liquid Stable Reagent into a 96-well plate. The plate was incubated for 300 seconds at 37°C and read at 500nm using Infinite 200 PRO (Tecan) reader. Both triglycerides and cholesterol measurements were performed in triplicate. Standard curves for interpolating rat samples were made based on a series of dilutions using triglyceride and cholesterol standards (TR22923, and TR13923, Thermo Fisher Scientific), respectively.

PKA Activity Assay

PKA activity was measured using a commercially available Protein Kinase A Activity Kit (ADI-EKS-390A, Enzo Life Sciences). LV free wall tissue (30-60 mg) was homogenized and prepared in the activated cell lysis buffer (provided in the kit). BCA assay was then performed to determine total protein concentration from each sample. 15µg of total protein was used for the assay. PKA activities of rat tissue samples were interpolated based on the standard curves.

RNA Extraction and Sequencing

LV free wall tissue (30-60 mg) was used for total RNA extraction. RNA was isolated using RNeasy plus mini kit (74134, Qiagen) according to the manufacturer's instructions. Briefly, frozen tissue was homogenized using a pellet pestle mixer (pellet pestle #12-141-361; motor 12-141-364; Fisher Scientific) in Buffer RLT Plus. Homogenates were then

transferred into gDNA Eliminator spin column with 2mL collection tube and centrifuged for 30 seconds at 10,000g. 1 volume of 70% EtOH was added to the flow through. 700µL of sample solution was transferred on to an RNeasy spin column with collection tube, and centrifuged for 15s at 10,000g. 500µL of RPE buffer was added and centrifuged for another 2 minutes at 10,000g. 30µL of total RNA was eluted from each sample from the RNeasy spin column into a new 1.5mL collection tube. Isolated RNA concentration in each sample was measured using NanoDrop One^{C} (Thermo Fisher Scientific). Genomic DNA contamination was not identified by 2% agarose electrophoresis gel. Illumina RNA sequencing was performed with total RNA (Water n=4; Binge n=4) at University of Chicago Genomics Facility.

Total cDNA Synthesis and qPCR Measurement

Total RNA (1 µg) was reverse transcribed using iScript ^{TM} Advanced cDNA synthesis kit (1725038, Bio-Rad). The resulting cDNA was diluted to 5ng/µL using nuclease-free water. Quantitative real time PCR was performed in triplicate using PowerUp SYBR Green Master mix (A25776, Thermo Fisher Scientific) with primers to specific genes (Table 1). Eno3, Rai1, Acadl, Lpl, Sln, Eln, and Actb primers were commercially available from the realtimeprimers.com. The primer sets FasN and Nppa have been previously published [62, 63]. No-template controls were performed to ensure that there was no reagent or primer contamination. The transcript fold changes for every gene expression were calculated using ΔΔCt method and compared to the housekeeping gene beta actin (atcb) values.

Symbol	Name	Forward	Reverse
FasN	Fatty acid synthase	GATGAAGAGGGACCATAAAGA TAAC	CCACTTGATGTGAGGGGAGAT
Eno3	Enolase	GAACTATCCCGTGGTCTCCA	CAATTGCAGGCCTTCTTCTC
Nppa	Naturetic peptide A	GAGCAAATCCCGTATACAGTGC	ATCTTCTACCGGCATCTTCTCC
Rai1	Retinoic acid induced 1	TACCCGTTCTCTCACAGCTC	AGAGTCTGGCTCCTTGGTTT
		ACAAAAGCCAGCATTGTAGC	CTGTTGACTCTGGCAGGACT
Acadl	Acyl-CoA dehydrogenase, long chain	ACCAGAGCTTTTGTGGACAG	GTTGGTACCACCGTAGATCG
		GAGCAGTTTATCCCCCAGAT	GTGATGAACACCTTGCTTCC
Lpl	Lipoprotein lipase	TTGGGATCCAGAAACCAGTA	GCAGGGAGTCAATGAAGAGA
		TGAAGACACAGCTGAGGACA	GATCACCACAAAGGTTTTGC
Sln	Sarcolipin	GGAGTTCTCACCCAGACCTT	AGGAGCACAGTGATCAGGAC
		GGTGTGCACTCAGAAGTCCT	ACAGAGCAGTGGAAGCTCAG
Eln	Elastin	TAGCTCCCTTGTTCTTGTGG	GTACTGCATGTGGGAAGGAC
		ACCTGGGTTTGGACTTTCTC	GGTCCCCAGAAGATCACTTT
Actb	Actin, beta	CACACTGTGCCCATCTATGA	CCGATAGTGATGACCTGACC

Table 1. List of Primers for Gene Expression Changes by Binge Alcohol Exposure. Primers used for qRT-PCR reactions for determining LV tissue key fatty acid metabolic gene expressions, and other important gene down regulations from RNA seq data (rat).

Statistics

All data were analyzed using Microsoft Excel and Prism 8.0.2 (Prism, CA). H&E data were measured using ImageJ. Food intake and the comparison of the H&E data were analyzed using two-tailed unpaired t-test, and a p-value of less than 0.05 was considered as significant. Comparisons between all Water, Binge, and Acute groups (BAC, corticosterone level) were analyzed using one-way ANOVA, followed by Tukey's post hoc test. Body mass measurements were analyzed using two way repeated measure

ANOVA with Tukey's multiple comparisons post hoc test. Water intake and the echo data (LVEDD, LVEDV, LVESD, LVESV, LVPWd, EF, FS, SV, CO and the E/A ratio) were analyzed using two way repeated measure ANOVA with Sidak's multiple comparisons post hoc test. The heart weight/ body weight ratio, passive tension, titin isoform comparisons, PKA activity, the pTnI/total TnI ratio, qPCR data, and the lipid prolife (plasma cholesterol, plasma triglyceride, tissue triglyceride level) between the Water and the Binge group were analyzed by two-tailed unpaired t-test. All values are presented as mean ± SEM.

CHAPTER FOUR

RESULTS

Adolescent Binge Alcohol Exposure Paradigm Establishment

In order to study the effects of binge alcohol consumption on the heart during adolescence, we utilized a well-established adolescent rat model of repeated binge pattern alcohol exposure with modifications. Seven days of initial handling period was to reduce the stress by human handling and gavage tools. The binge pattern alcohol exposure protocol was performed at the age of PND37 to PND 44. Plasma blood alcohol content (BAC) was measured from the collected truck blood one hour within the last gavage. Both the Binge group and the Acute group reached expected BAC of average 0.08 g/dL, and Water control rats had BAC of 0 g/dL (Water n=16, Binge n=15, Acute n=8; $p<0.0001$ Water vs. Binge, and Water vs. Acute; $p<0.0001$, by one way ANOVA with Tukey's multiple comparisons post hoc test; Figure 5A). The Binge and the Acute rats had similar BAC ($p=0.1149$). The adrenal gland secretes glucocorticoid hormones as an essential physiological response to alcohol stress. Glucocorticoid hormones, cortisol in humans and corticosterone in rats and mice, regulate many processes in the body including the mobilization of energy stores and immune function [64, 65]. Plasma corticosterone concentration was also measured in all three groups to determine the stress levels. The Acute group had a significant increase in corticosterone level, suggesting the very first binge dose of alcohol caused acute stress to the rats ($p=0.0144$

Water vs. Acute; p=0.1191 Water vs. Binge; p=0.5718 Binge vs. Acute; p=0.0169, by one way ANOVA with Tukey's multiple comparisons post hoc test, Figure 5B). The Binge rats had gradually reduced the stress level with the repeated alcohol exposure. The Water and the Binge groups had similar overall food intake after the 8-day treatment (Water n=4 pairs, Binge n=4 pairs; p=0.1598 by unpaired t-test; Figure 5C). The Binge rats also had similar water intake compared with the Water control rats during the treatment (Water n=4 pairs, Binge n=4 pairs; $p_{interaction}$=0.0066, $p_{source\ of\ variation\text{-}Alcohol\ treatment}$=0.4329, $p_{source\ of\ variation\text{-}Time}$=0.2092 by two way repeated measure ANOVA with Sidak's multiple comparisons post hoc test; Figure 5D). Water and food intake of the Acute group was not measured since the rats only received alcohol at the last gavage. All three groups had similar body mass increase during the treatment (average body mass on PND38 to PND44: Water n=21, 156.5 ± 4.0 g to 225.7 ± 5.6 g SEM; Binge n=22, 161.9 ± 2.9g to 230.0 ± 4.0 g SEM; Acute n=13, 152.5 ± 4.1 g to 222 ± 5.5 g SEM; $p_{interaction}$=0.9325, $p_{source\ of\ variation\text{-}Alcohol\ treatment}$=0.4683, $p_{source\ of\ variation\text{-}Time}$<0.0001 by two way repeated measure ANOVA with Tukey's multiple comparisons post hoc test; Figure 5E).

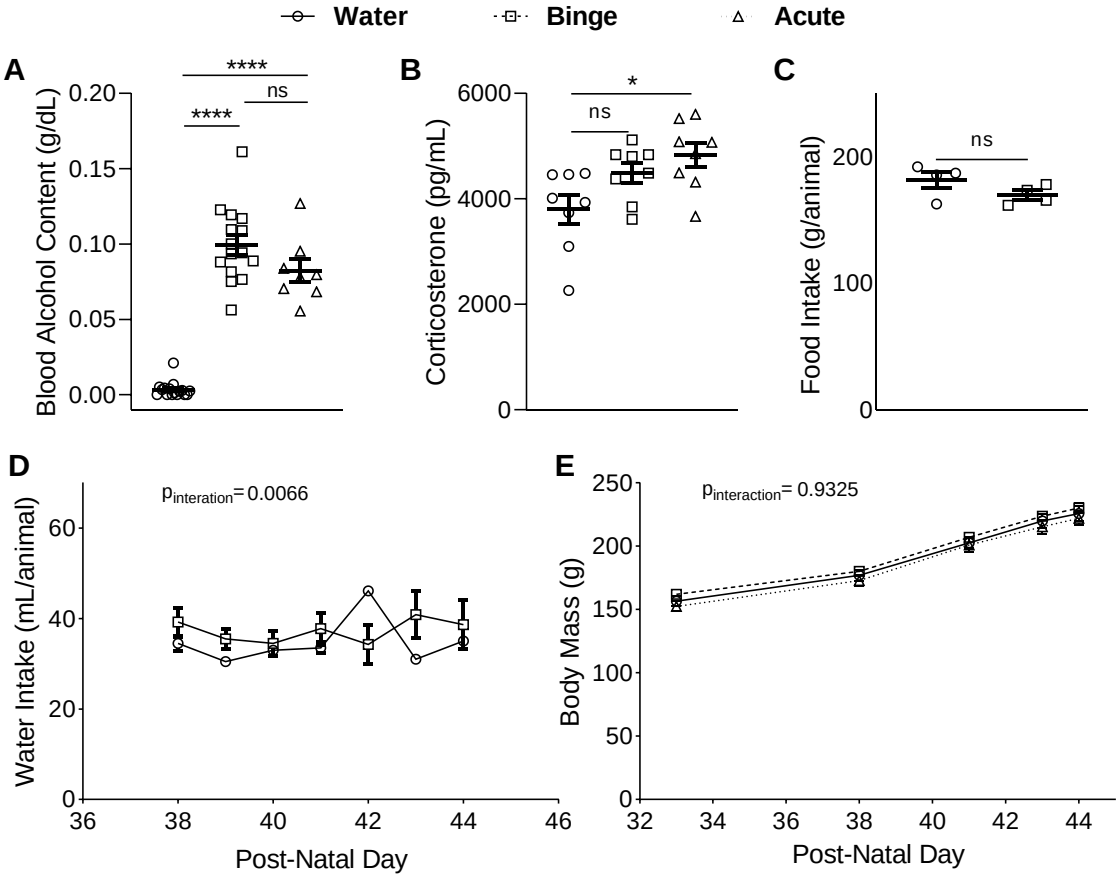

Figure 5. All Three Groups had Expected BAC and Corticosterone Levels, and all Groups had Similar Food and Water Intake and Body Growth. Three groups: Water (empty circle, solid line), Binge (empty square, dash line), and Acute (empty triangle, dotted line). (A) Binge and Acute groups reached blood alcohol content (BAC) of expected 0.08 g/dL. Water group had 0 g/dL BAC level (****p<0.0001 Water vs. Binge, ****p<0.0001 Water vs. Acute; p=0.1003 Binge vs. Acute; Water n=16, Binge n=15, Acute n=8; p<0.0001 by ordinary one way ANOVA with Tukey's multiple comparisons post hoc test). (B) Acute group had increased plasma corticosterone level than the Water group (*p<0.5 Water vs. Acute; Water n=8, Binge n=8, Acute n=8; p=0.0169 by ordinary one way ANOVA with Tukey's multiple comparisons post hoc test). (C) Both Water and Binge groups had similar amount of food intake (Water n=4 pairs, Binge n=4 pairs, p=0.16 by unpaired t-test). (D) Both Water and Binge groups had similar amount of water intake (Water n=4 pairs, Binge n=4 pairs; $p_{interaction}$=0.0066, by two way repeated measure ANOVA with Sidak's multiple comparisons post hoc test). (E) All three groups had similar rate of growth during the 8-day treatment ($p_{interaction}$=0.9325, Water n=20, Binge n=21, Acute n=13; by two way repeated measure ANOVA with Tukey's multiple comparisons post hoc test).

Cardiac Structural and Functional Changes by Binge Alcohol Exposure

We hypothesized that binge pattern alcohol exposure in adolescence would decrease cardiac function and increase pathologic hypertrophy, as previously shown in adult alcoholic cardiomyopathy patients [3]. To assess the effects on heart functional and

structural changes during adolescence, I retrieved the raw echo measurements data (M mode and Doppler) by our facility animal surgeon Dr. Quan Cao from baseline (prehandle period) and at post treatment (within one hour after the last dose). Firstly, no differences in echo parameters were found between the Water and Binge groups at baseline in all parameters (Figure 6). While both groups had increased LV end-diastolic diameters (LVEDDs) after 8-day treatment as they age, the Water group had larger LVEDDs compared to the Binge group at post treatment (baseline vs. post: $p<0.0001$ Water, $p<0.0001$ Binge; at post treatment: $p=0.0072$ Water vs. Binge; $p_{interaction}=0.0015$, by two way repeated measure ANOVA with Sidak's multiple comparisons post hoc test; Figure 6A, B). By calculation using the Vevo 2100 analytical software, both groups increased LV end-diastolic volumes (LVEDVs) with time (baseline vs. post: $p<0.0001$ Water, $p<0.0001$ Binge), but the Binge group had smaller LVEDV compared to the Water group at post treatment ($p=0.003$ at post treatment, 240±8.41μL vs. 205.3±6.40μL, Water vs. Binge; $p_{interaction}=0.0008$ significant by two way repeated measure ANOVA with Sidak's multiple comparisons post hoc test; Figure 6C). Smaller end diastolic dimensions post treatment suggest the possibility of slower heart growth from adolescent binge alcohol exposure.

The Water group increased LV end-systolic diameters (LVESDs) after the 8-day treatment, whereas the Binge group kept similar LVESDs (baseline vs. post: $n=14$, $p=0.0015$ Water; $n=14$, $p=0.2852$ Binge). The Water group had bigger LVESD compared to the Binge group at post treatment ($p=0.007$ Water vs. Binge; $p_{interaction}=0.0048$ significant by two way repeated measure ANOVA with Sidak's multiple comparisons post hoc test; Figure 6A, D). Based on calculation with the measured systolic diameters, Water rats had an increase in LV end-systolic volumes (LVESVs) with time ($p=0.0145$, $n=14$),

and at post treatment Water group had larger LVESVs than the Binge group (p=0.0278, $p_{interaction}$=0.0073 by repeated measure two way ANOVA with Sidak's multiple comparisons post hoc test; Figure 6E).

Ejection fraction (EF) is commonly assessed as a clinical index for evaluating the contractile function of the heart. We analyzed the EF for both groups of rats. Here, EF was calculated using the equation EF = [(EDV-ESV)/EDV)]*100%. The Water group remained similar EF at both echo time points (Water baseline vs. post: 79.8 ± 1.5 % vs. 81.6 ± 1.7 %, p=0.4773, n=14), but opposite as we hypothesized, the EF of the Binge group significantly increase post treatment (Binge baseline vs. post: 79.0 ± 1.3% vs. 85.9 ± 1.5%, p=0.0005, n=14; $p_{interaction}$=0.0342 by two way repeated measure ANOVA with Sidak's multiple comparisons post hoc test; Figure 6F). Next, we analyzed the fractional shortening (FS) of the two groups. FS is the fraction of a diastolic dimension that is reduced in systole, and is a similar measurement to EF. The Binge group had an increase in FS post treatment (Binge baseline vs. post: 48.7 ± 1.4% vs. 57.5 ± 1.7%, p=0.0001; n=14 Water, n=14 Binge; $p_{interaction}$=0.0173 by two way repeated measure ANOVA with Sidak's multiple comparisons post hoc test; Figure 6G). In addition, both groups increased LV posterior wall diameter during diastole (LVPWd, baseline to post: Water 1.55 ± 0.04 mm to 1.71 ± 0.05 mm, p=0.018, n=15; Binge 1.64 ± 0.05 to 1.88 ± 0.07 mm, p=0.0005, n=15). The Binge group had larger LVPWd comparing to the Water group post treatment, indicating thickening of the LV chamber with binge alcohol exposure (p=0.0285 Water vs. Binge; $p_{interaction}$=0.3272, $p_{source\ of\ variantion\text{-}Time}$ <0.0001, $p_{source\ of\ variation\text{-}Alcohol\ treatment}$ =0.0242 by two way repeated measure ANOVA with Sidak's multiple comparisons post hoc test;

Figure 6H). Higher EF and FS indicates increased systolic function in the Binge group after binge alcohol exposure compared to the Water group.

The increase in systolic and diastolic parameters in the Water group represents the normal growth of the heart over 8 days in adolescent rats. M-mode echo data showed smaller diastolic dimensions but increased heart contractility in the Binge group post treatment. Next we wanted to compare overall cardiac output (CO) of two groups, first we had to calculate stroke volume (SV) for the two groups. Using the equation of SV = EDV – ESV, both the Water group and the Binge group increased SV post treatment (baseline to post: 128.7 ± 5.7 μL to 196.8 ± 7.0 μL, n=15, Water; 126.0 ± 3.6 μL to 176.2 ± 6.0 μL, n=14, Binge; $p<0.0001$ for Water and Binge, respectively). The Water group had bigger SV than the Binge group at post treatment ($p=0.0319$; $p_{interaction}=0.0069$ by two way repeated measure ANOVA with Sidak's multiple comparisons post hoc test; Figure 6I). Heart rate (HR) was measured when rats were under stable 2% isoflurane during each echo procedure. Using the equation CO = HR * SV, two groups maintained similar increase in CO after the treatment (baseline vs. post: Water 56.5 ± 3.0 mL/min vs. 81.1 ± 3.6 mL/min, n=13; Binge 56.9 ± 1.8 mL/min vs. 81.9 ± 4.4 mL/min, n=13; $p<0.0001$ for Water and Binge, respectively; $p_{source\ of\ variation\text{-}Time}<0.0001$ analyzed by two way repeated measure ANOVA with Sidak's multiple comparisons post hoc test; Figure 6J).

M-mode echo data showed binge alcohol increased systolic function in adolescents, as the opposite results of what we originally anticipated from the adult patients. Sympathetic activation is known to be stimulated in adult alcoholic cardiomyopathy patients, and it can temporarily restore heart function [3]. Adolescent rats

had smaller diastolic dimensions but still were able to maintain the same CO as the Water controls post binge alcohol exposure. We then hypothesized that the 8-day binge alcohol exposure in adolescence induced compensatory mechanism by sympathetic activation to maintain cardiac output (CO) by increasing systolic function.

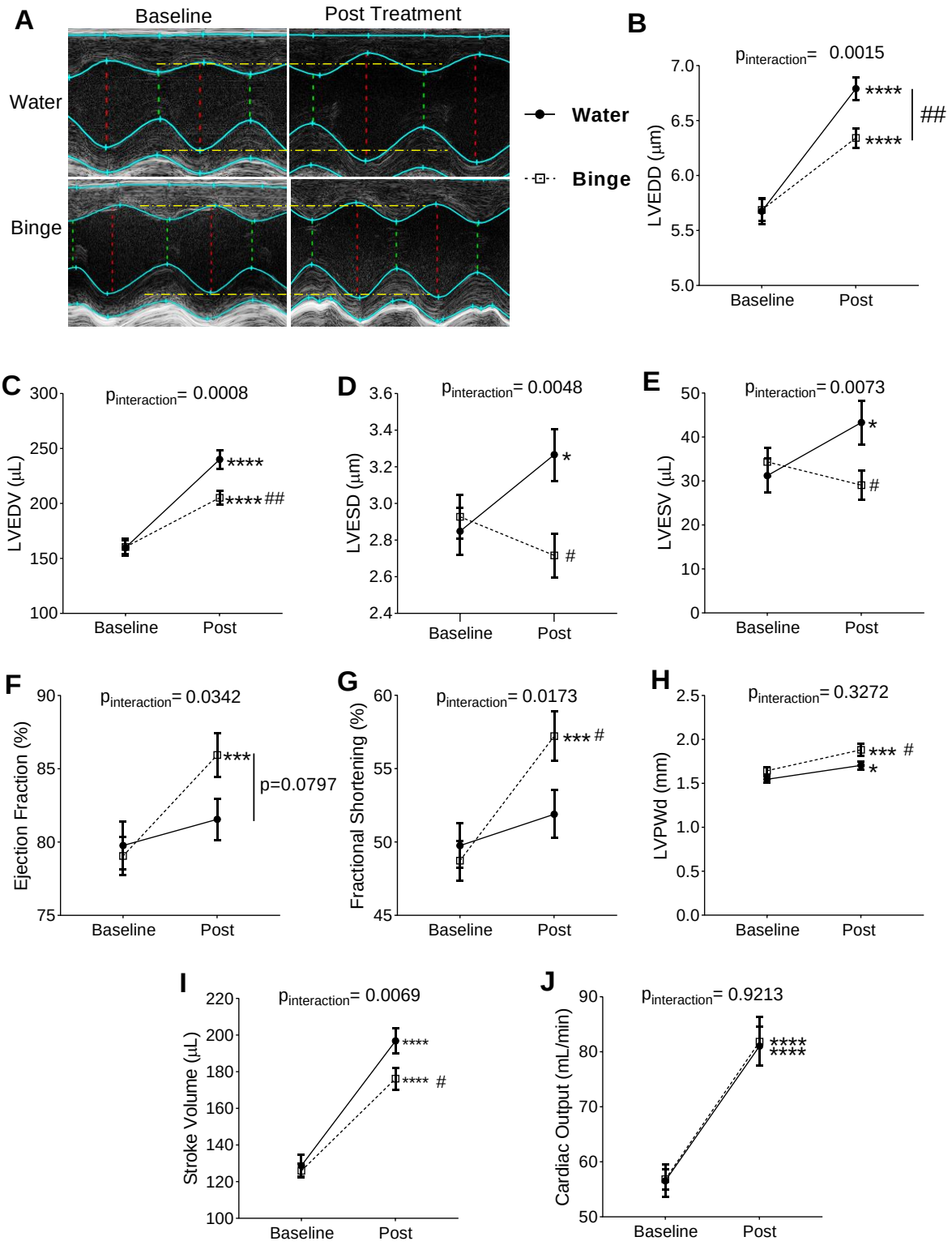
A
Baseline
Post Treatment
Water
Binge
Water
Binge
B
p interaction= 0.0015
LVEDD (µm)
****
****
##
Baseline
Post
C
p interaction= 0.0008
LVEDV (µL)
****
****##
D
p interaction= 0.0048
LVESD (µm)
*
#
E
p interaction= 0.0073
LVESV (µL)
*
#
F
p interaction= 0.0342
Ejection Fraction (%)
***
p=0.0797
G
p interaction= 0.0173
Fractional Shortening (%)
*** #
H
p interaction= 0.3272
LVPWd (mm)
*** #
*
I
p interaction= 0.0069
Stroke Volume (µL)
****
**** #
J
p interaction= 0.9213
Cardiac Output (mL/min)
****
****

Figure 6. Motion Mode Echocardiograph Parameter Changes. Water (bold circle, straight line) and Binge (empty square, dashed line) (A) Representative M-Mode echocardiograph images of Water and Binge group at both baseline and post treatment measurements. Distance between dotted lines represent LVESD; distance between flat lines represent LVEDD. (B, C) Both groups had increased LV end diastolic diameters and volume post treatment than baseline. At post treatment, Binge group had less of diastolic diameters (B) and volume (C) comparing to water controls, indicating altered ventricular structure after binge exposure. (D) Water group had significant increase in LV end-systolic diameters post treatment than baseline, while Binge group remained similar LVESD. LVESD of Water rats at post treatment is bigger than binge rats. (E) Water group has a trend towards bigger end systolic volume at post treatment than Binge, indicating binge alcohol exposure leads to stronger systolic contraction. (F) Binge group had increased ejection fraction than Water group after binge alcohol treatment. (G) Binge group had increased fractional shortening than Water group after binge alcohol treatment. (H) Water group had similar LV posterior wall dimensions at both time points, but binge group had significant increase in LVPWd at post treatment. (I) Both groups had increased stroke volume at post treatment than baseline. (J) Water and Binge groups maintained similar cardiac output. *p<0.05 vs. baseline, **p<0.01 vs. baseline, ***p <0.001 vs. baseline, ****p<0.0001 vs. baseline, #p<0.05 vs. water at post treatment, #p<0.01 vs. water at post treatment, $p_{interaction}$ in different parameters by two way repeated measure ANOVA with Sidak's multiple comparisons post hoc test.

Because the Acute group had no difference found in post treatment echoes comparing to Water group (Figure 7), only Water and Binge rats echo data are compared in the results section.

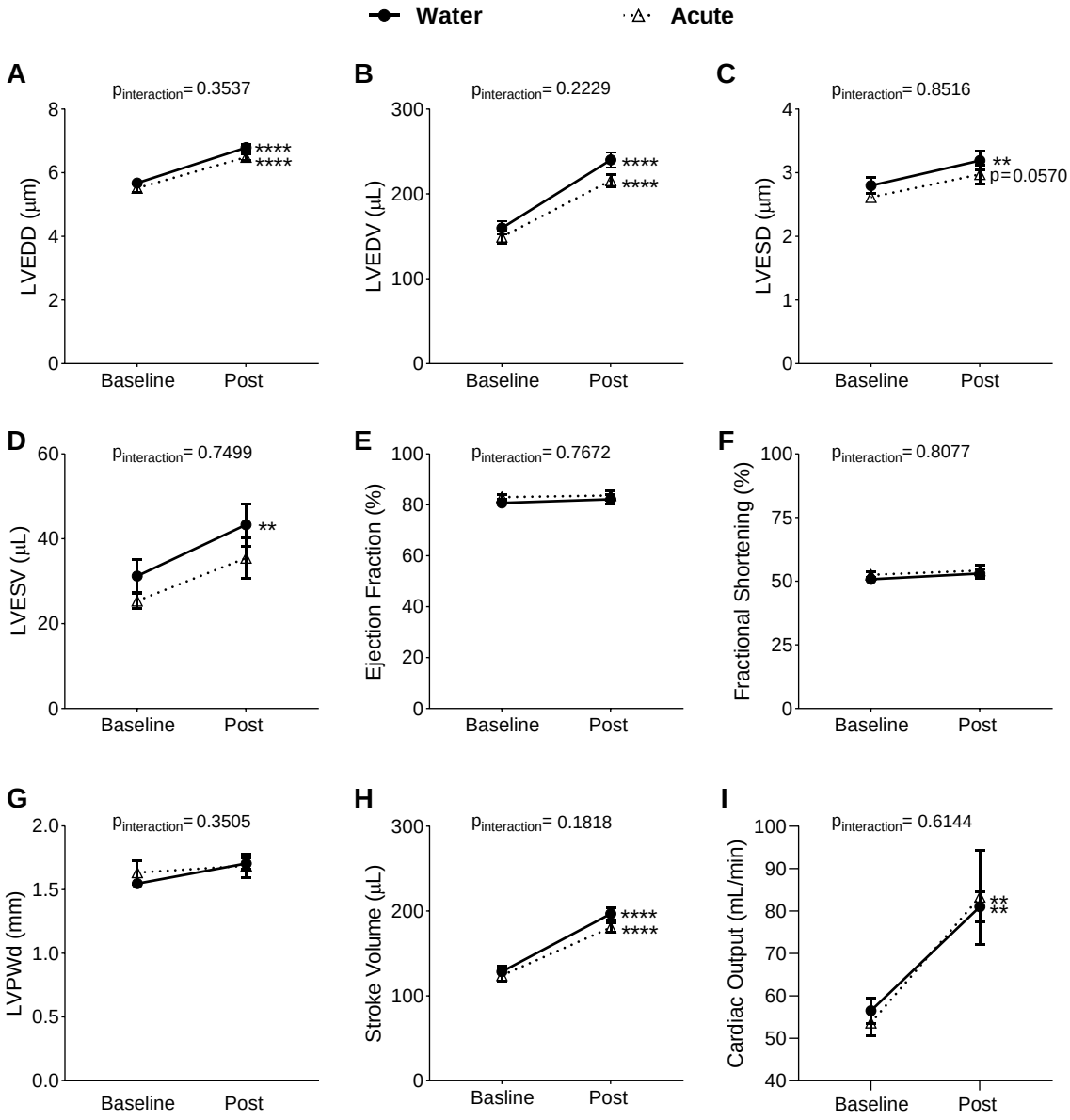

Figure 7. M-Mode Echo Data Comparisons between the Water and the Acute Groups. (A, B) The Water (bolded circle, straight line) and Acute rats (empty triangle, dotted line) had steady increase in diastolic diameters (A) and volumes (B) post treatment comparing their own baseline, indicating heart growth during adolescence. Both groups had similar diastolic diameters (A) and volumes (B) between groups at both time point measurements. (C, D) The Water and Acute rats had similar systolic diameters (C) and volumes (D) post treatment comparing to their own baseline respectively, and between groups at both time point measurements. (E) Both the Water and the Acute rats had stable normal EF at two time points. (F) Both the Water and the Acute rats had stable normal FS at two time points. (G) Both the Water and the Acute group had similar posterior wall thickness. (H) Both the Water and the Acute group had increase SV post treatment comparing their own baseline. No difference in SV found between groups post treatment. (I) Both groups increased CO with time. Both groups had similar CO at post treatment echo. Water n=8, Acute n=8; *p<0.05, **p<0.01, ***p<0.001, and ****p<0.0001 by two way repeated measure ANOVA with Sidak's multiple comparisons post hoc test.

We measured the heart weight post treatment using an analytical balance (XS64, Mettler Toledo) in another binge alcohol exposure cohort, which was kindly provided from Dr. Toni Pak's lab. Heart weight to body weight ratio of each group was similar between the Water rats and the Binge rats (Water n=5, Binge n=6; p=0.2231 by unpaired t-test; Figure 8).

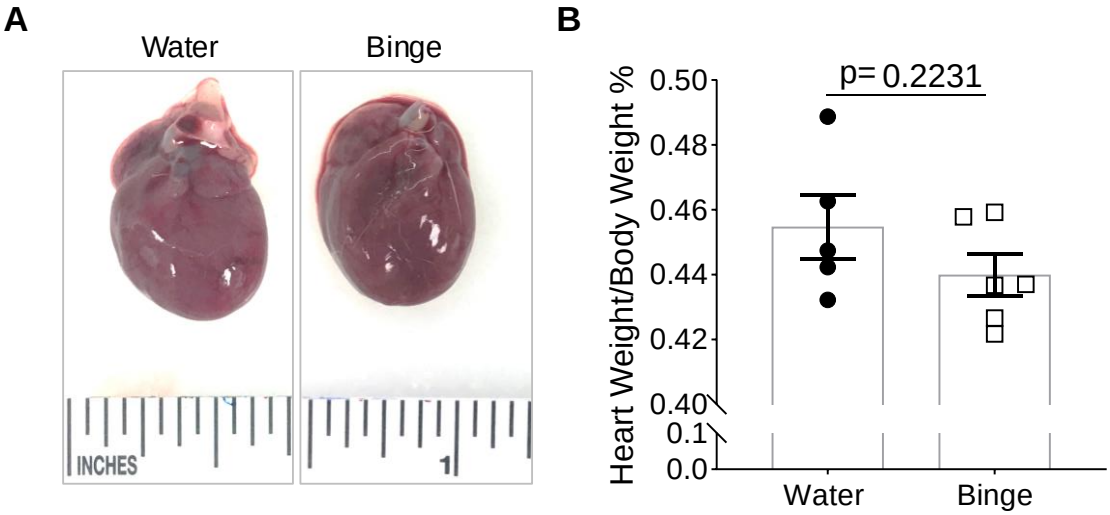

Figure 8. Heart Weight Comparisons between the Water and the Binge Groups Post Treatment. (A) Representative heart images of the Water and the Binge rats at PND44 immediately after euthanasia. (B) Quantitative analysis of the ratio of heart weight to body weight in two groups (Water n=5, Binge n=6; p=0.2231 by unpaired t-test).

Binge Alcohol Exposure Altered Normal Cardiomyocyte Remodeling

Because of the changes we observed from the M-mode echo, we then investigated the individual cardiomyocyte morphology using H&E staining. We hypothesized that binge pattern alcohol consumption increases cardiomyocyte hypertrophy in adolescence. We assumed all rats had similar cardiomyocyte morphology at baseline conditions. In order to study the effects after binge alcohol exposure, we compared the cardiomyocytes at post treatment between two groups. Rat LVs were preserved for H&E staining in 10%

formalin immediately after euthanasia at PND44 (Water n=4, Binge n=4). Cardiomyocytes images were captured at base, middle, and apex of the LV using a light microscope (x100 and x400). Multiple representative cardiomyocytes were measured for concentric hypertrophy and eccentric hypertrophy analysis. Measurements were analyzed and compared by 3 blinded individuals separately. After the 8-day treatment, Binge group had increased average cardiomyocyte cross-section area at the middle and the base of LV compared to the Water group (Apex: $p=0.97$, $305.9 \pm 11.0 \mu m^2$ vs. $305.4 \pm 11.0 \mu m^2$, $n_{\#cells}=50$ vs. $n_{\#cells}=68$, Water vs. Binge; Middle: $p=0.0316$, $276.8 \pm 5.6 \mu m^2$ vs. $295.2 \pm 5.6 \mu m^2$, $n_{\#cells}=282$ vs. $n_{\#cells}=239$, Water vs. Binge; Base: $p=0.012$, $293.7 \pm 6.9 \mu m^2$ vs. $320.1 \pm 8.0 \mu m^2$, $n_{\#cells}=184$ vs. $n_{\#cells}=182$, Water vs. Binge; by unpaired t-test; Figure 9A, C). Then we measured the longitudinal lengths of the cardiomyocytes (Figure 9B; white arrows point at intercalated disks, and the length of one cell is measured between two intercalated disks). The Binge group had longer cardiomyocyte lengths than the Water group at the Apex (Apex: $p=0.0002$, $n_{\#cells}=62$ vs. $n_{\#cells}=41$; $69.2 \pm 1.9 \mu m$ SEM vs. $81.5 \pm 2.7 \mu m$ SEM, Water vs. Binge; Middle: $p=0.42$, $n_{\#cells}=81$ vs. $n_{\#cells}= 46$, $71.6 \pm 2.1 \mu m$ SEM vs. $74.3 \pm 2.3 \mu m$ SEM, Water vs. Binge; Base: $p=0.53$, $n_{\#cells}=58$ vs. $n_{\#cells}=61$, $82.1 \pm 2.6 \mu m$ vs. $79.9 \pm 2.3 \mu m$, Water vs. Binge; by unpaired t-test; Figure 9D). Adolescent binge alcohol exposure increased cardiomyocyte eccentric hypertrophy at the apex and increased concentric hypertrophy at the middle and base positions in the LV. The difference of hypertrophic increases at different LV positions suggests binge pattern alcohol altered cardiac structure after only 8 days.

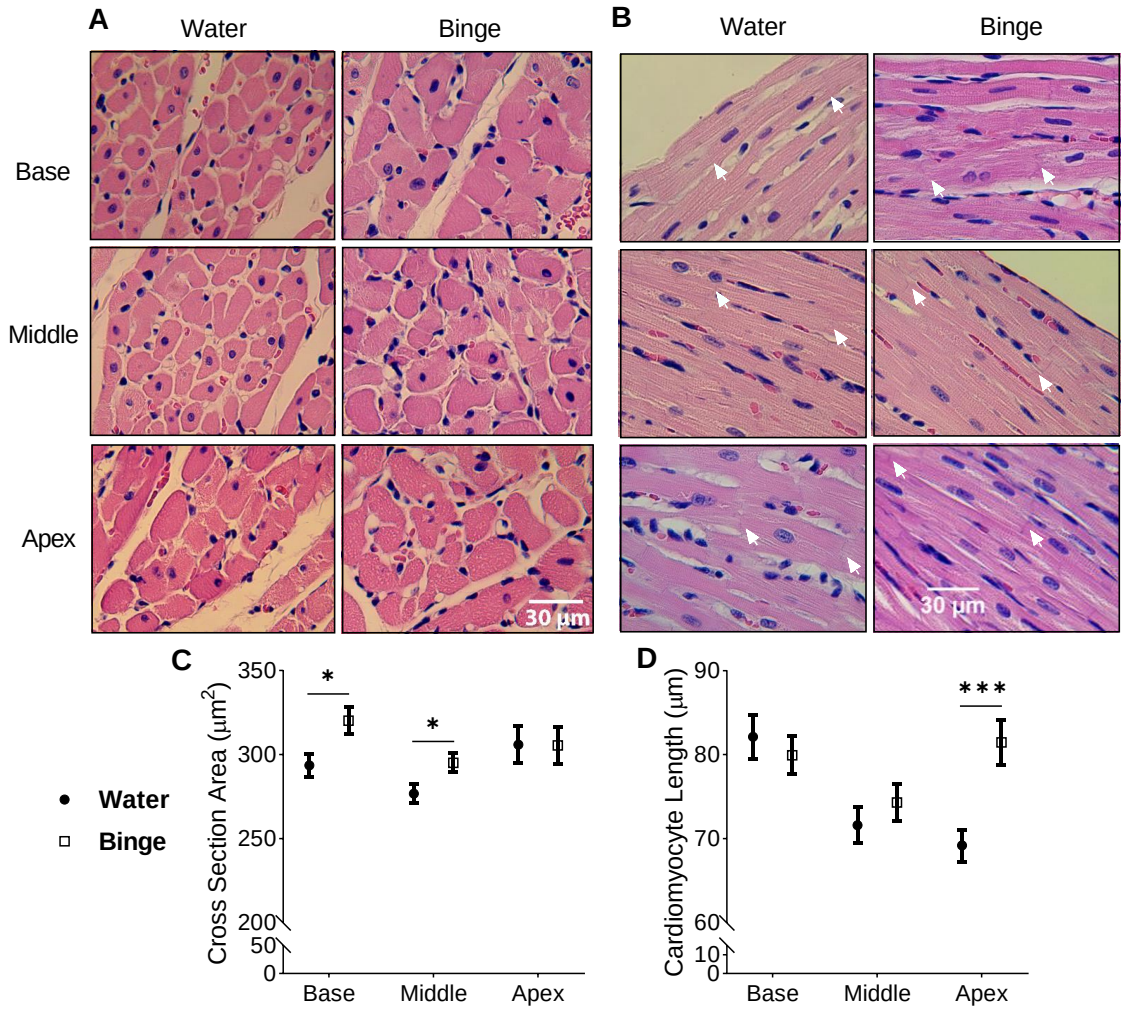

Figure 9. Binge Alcohol Exposure Alters Cardiomyocyte Concentric and Eccentric Hypertrophy. (A) Representative H&E histological images of LV cardiomyocyte cross-section areas at locations Base, Middle, and Apex. (B) Binge rats had increased concentric hypertrophy at the middle and base of LV after binge alcohol exposure than Water rats. Two groups had similar cross section areas at Apex. (C) Representative H&E histological images of LV cardiomyocyte Longitudinal section areas at locations Base, Middle, and Apex. White arrows point at intercalated disks. Each pair of arrows represents measurement of each individual cardiomyocyte length between intercalated disks. (D) Binge group had increased eccentric hypertrophy at Apex of LV than Water group (*p<0.05, ***p<0.001 by unpaired t-test).

Diastolic Consequences after Binge Alcohol Exposure Decreased in Adolescence

Doppler echocardiograph (Doppler) was measured at the same time as the M-mode for baseline and post-treatment comparison. Doppler measures E to A ratio (the ratio of peak velocity from early ventricular filling to peak velocity from atrial contraction during diastole), which is a marker assessing diastolic function. The Water group

increased E/A ratio with time, as their hearts are getting more compliant during normal adolescent growth (p=0.014, n=16, 2.02 vs. 2.5, SE of diff. = 0.20, baseline vs. post). The binge group maintained the similar baseline compliance post treatment (p=0.717, n=16, 1.98 vs. 2.11, SE of diff. = 0.21, baseline vs. post; by two way repeated measure ANOVA with Sidak's multiple comparisons post hoc test; Figure 10A). Binge group still had an E/A ratio value within a healthy range (E/A >2 for young adults, based on ASE/EACVI guidelines and standards [32]), but we were very interested to understand the reason for the smaller E/A ratio in the Binge rats compared to the Water controls at post treatment. We then studied the possible changes that could lead to the difference in diastolic function. Diastolic dysfunction is linked to a decrease in LV compliance. Compliance is determined by both cardiomyocyte passive tension and extracellular matrix protein compositions. In alcoholic cardiomyopathy patients, both increase in passive tension and fibrosis by ECM remodeling have been studied to cause decrease in diastolic E/A ratios [66, 67]. We first hypothesized that adolescent binge alcohol exposure reduces heart diastolic compliance by increasing cardiomyocyte passive tension. Myofilament passive tension was measured by our previous lab member Dr. Maxime Heroux, and she found that the Binge group cardiomyocytes had significantly higher passive tension compared to the Water group at every sarcomere length (1.8-2.4 μm). Binge alcohol exposure increased cardiomyocyte passive stiffness after only 8-days of treatment in adolescent rats. Increased passive stiffness is a common characteristic of diastolic dysfunction, which can eventually cause heart failure. A stiff LV myocardium can fill with less blood, thus it also agrees with the M-mode echo data showing the smaller LVEDV in the Binge group compared to the Water group at post treatment.

Titin is a spring-like protein that connects the sarcomere Z line to M line and is responsible for muscle elasticity. The switch in expression levels between isoforms N2BA (longer and more compliant titin) and N2B (the shorter and stiffer titin) was found in patients with diastolic dysfunction [51]. Titin modifications can also be responsible for cardiomyocyte passive stiffness [68]. In order to test whether the increased passive stiffness was due to titin isoform switching in Binge group, we modified a specialized titin gel to separate the two isoforms by size (Figure 10D). We then sent more myofilament samples to our collaborator Dr. Charles Chung's lab in Wyane State University for titin isoform visualization. However, after analyzing the results we received from Wyane State, the Binge group did not show any differences in titin isoforms (Figure 10E), degradation (Figure 10F), or overall protein expression (Figure 10G). One possibility is that 8-day of binge alcohol exposure is not long enough for the large titin protein turnover, which has half-life of 3.5 days [69].

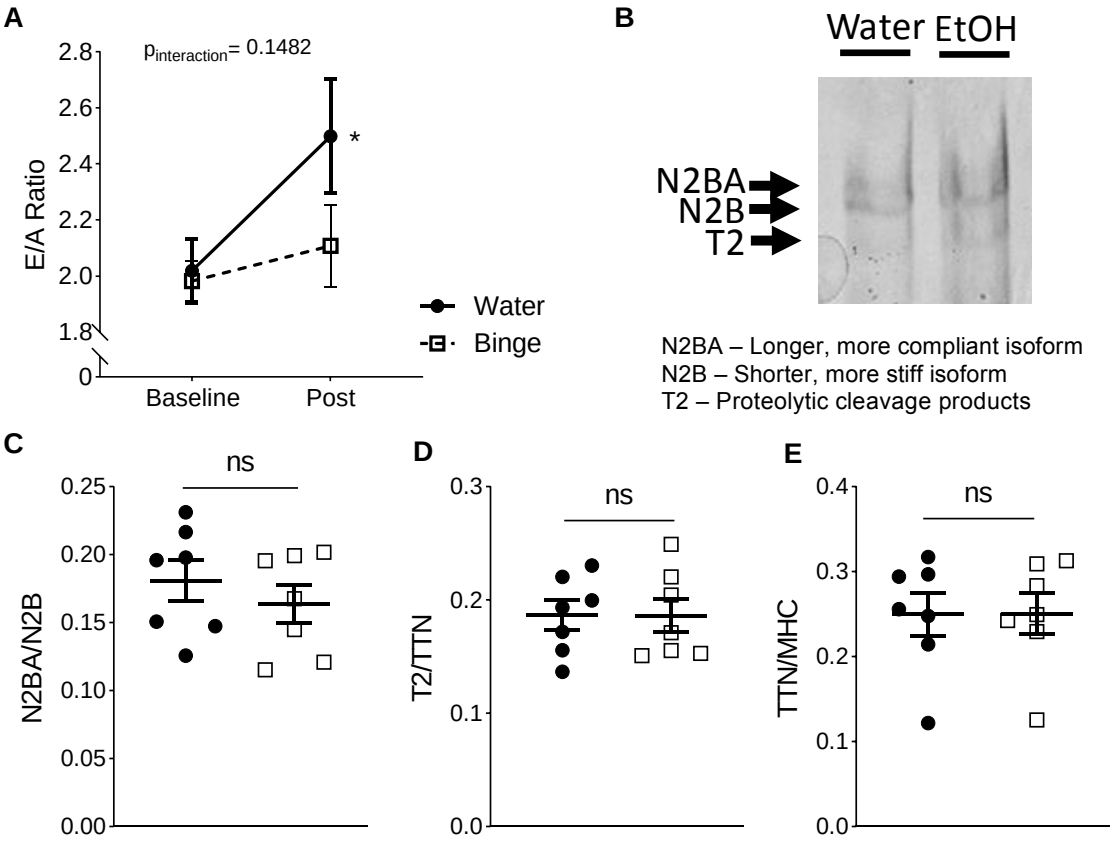

Figure 10. Binge Alcohol Effects on Diastolic Function. (A) E/A ratio showing a trend towards decreased diastolic function in Binge group. (B) Specialized titin gel showing two titin isoforms in both Water and Binge groups. (C) No difference found between the ratio of N2BA over N2B in two groups. (D) No difference found between the ratio of proteolytic cleavage products (T2) over total titin (TTN) in two groups. (E) No difference is found between the ratio of TTN over myosin heavy chain (MHC) control in Water and Binge groups.

We also measured the E/A ratio of the Acute group, and the Acute group had similar E/A ratio increase as the Water group. (Water n=8, Acute n=8; $p_{source\ of\ viariation\text{-}Alcohol\ treatment}$=0.703; p=0.025 Acute baseline vs. post; $p_{source\ of\ viariation\text{-}time}$= 0.0057 by two way repeated measure ANOVA with Sidak's multiple comparisons post hoc test; Figure11).

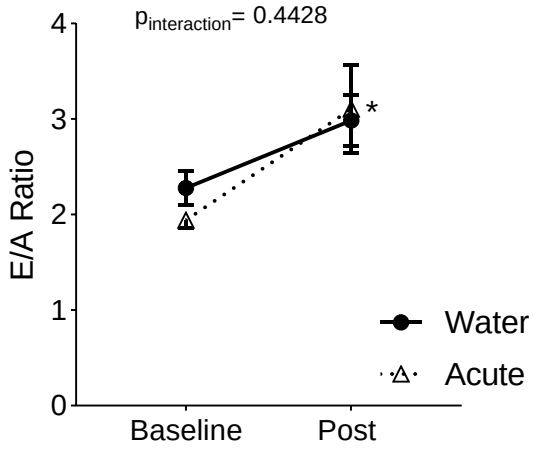

Figure 11. Doppler Echo Results Comparison between Water and Acute Rats. Acute group (empty triangle, dotted line) showed increase in E/A ratio with time. Water (bold circle, straight line) n=8, Acute n=8; *p<0.05 Acute baseline vs. post; Water baseline vs. post; by two way repeated measure ANOVA with Sidak's multiple comparisons post hoc test.

The Binge Group Increased Beta-Adrenergic Signaling Protein Phosphorylation

We were interested in determining the possible signaling mechanism that led to increased systolic function in the Binge rats. Beta-adrenergic signaling constantly regulates systolic function. Activation of beta-adrenergic signaling increases systolic contraction and HR, and maintains CO under stress conditions [10]. We hypothesized that binge alcohol exposure increased beta-adrenergic stimulation in adolescent rats. Firstly, we measured the key beta-adrenergic downstream kinase PKA activity using a commercially available kit. However, The PKA activity assay did not detect the difference between the Water and Binge rats (Water n=6, Binge n=7; p=0.6467 by unpaired t-test; Figure 12A). Although there was a trend towards a 15-20% increase, we think that the assay was not sensitive enough to detect such a modest increase. Therefore, we measured beta-adrenergic pathway protein cardiac Troponin I (TnI) phosphorylation (Figure 12B). TnI, as an inhibitory unit of the troponin complex, inhibits actin and myosin

interaction during diastole [70]. TnI at S22/23 (S23/24 if the initiating methionine is counted) is commonly phosphorylated by PKA. TnI phosphorylation decreases myofilament Ca^{2+} sensitivity and accelerates heart relaxation [70]. The Binge group had a 22% increase in TnI phosphorylation at the S22/23 sites compared to the Water group (ratio of green channel pTnI at S22/23 site to red channel total TnI; Water n=9, Binge n=15; p=0.0472 by unpaired t-test; Figure 12C).

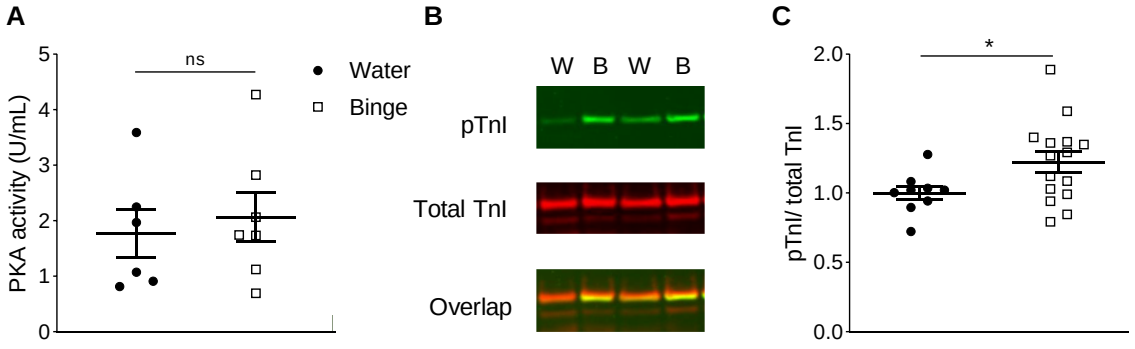

Figure 12. Binge Alcohol Exposure Increased B-Adrenergic Signaling Pathway Protein Phosphorylation. (A) Water and Binge group had variable PKA activity within the groups, although there might be a trend towards 15-20 % increase in the Binge group (Water n=6, Binge n=7; p=0.6467 by unpaired t-test). (B) Western blot image of phosphorylated cardiac TnI at S22/23 and total cTnI. (C) Binge alcohol exposure increased cTnI phosphorylation. Water n=9, Binge n=15; *p<0.05 by unpaired t-test.

Binge Alcohol Exposure Interrupted Regulatory Gene Expressions in the Heart

The effects of binge alcohol consumption on the adolescent heart are almost entirely unknown, so we next examined genome wide mRNA expression changes in the two groups (Water n=4, Binge n=4). Total mRNA was extracted and prepared for RNA seq from LV myocardium, and we analyzed the genes with significant fold changes after binge alcohol exposure (Table 1, Figure 13A). Interestingly, mRNA showed down regulation of several genes for fatty acid metabolism in the Binge group, such as fatty

acid synthase (fasn), Enolase 3 (eno3), lipid lipase (lpl), and Acetyl-CoA dehydrogenase (acadl) (Table 3). We performed quantitative real time PCR with primer sets specific to those genes, respectively (Table 2). Binge group qPCR results did not show significant expression changes in those genes compared to the Water group (Water n=6, Binge n=6; Figure 13B). However, repetitive experiments on more animals need to be done for the qPCR analysis. RNA seq suggested other important gene down regulations such as sarcolipin (Sln), retinoic acid induced 1 (Rai1), and natriuretic peptide A (Nppa). Sarcolipin is a small trans-membrane protein that regulates sarcoplasmic reticulum calcium ATPase, and ablation of sarcolipin increases calcium transport and atrial contractility [71]. Rai1 is one of the regulatory genes that is responsible for circadian rhythm and brain development [72]. Natriuretic peptide A production is stimulated with increased systolic blood pressure to decrease blood pressure. The qPCR results supported the trend of decreased fold change in nppa and sln (Figure 13C). Both groups had similar concentrations of triglyceride and cholesterol, indicating normal liver functions (Figure 13D, E). Because the RNA seq data indicated changes in some metabolic gene expressions with binge alcohol exposure, we further examined the LV muscle tissue triglyceride level. No difference was found in tissue triglyceride level between both groups (Figure 13F).

1. Gene Identifiers	2. mean normalised counts, averaged over all samples from both conditions	3. the logarithm (to basis 2) of the fold change (See the note in inputs section)	3a. Fold change	4. standard error estimate for the log2 fold change estimate	5. Wald statistic	6. p value for the statistical significance of this change	-Log10 p-value	7. p value adjusted for multiple testing with the Benjamini-Hochberg procedure which controls false discovery rate (FDR)
Fasn	12.24736	-2.1999	0.217653	0.446678	-4.92502	8.44E-07	6.073901	0.000644
Sln	14.53553	-2.01824	0.246859	0.417087	-4.8389	1.31E-06	5.884183	0.000664
Rai1	36.04632	-1.77878	0.29143	0.357908	-4.96994	6.70E-07	6.174099	0.000644
Nppa	227.3007	-1.59234	0.331633	0.448542	-3.55004	0.000385	3.414339	0.074035
Eln	52.14446	-1.33045	0.397644	0.338314	-3.93259	8.40E-05	4.075529	0.03206
Scd1	23.26321	-1.14067	0.453548	0.414662	-2.75085	0.005944	2.225912	0.232583
Acly	5.052024	-0.98143	0.506478	0.450011	-2.1809	0.029191	1.534757	NA
Lpl	188.4118	0.638076	1.556252	0.218135	2.925147	0.003443	2.463071	0.164185
Cd36	23.95569	0.87589	1.83514	0.310713	2.818972	0.004818	2.317154	0.198701
Eno3	17.87893	0.916038	1.886926	0.372983	2.455976	0.01405	1.852316	0.400225

Table 2. RNA Seq Data. Expression changes in several key myocardial metabolism genes and myofilament structural genes.

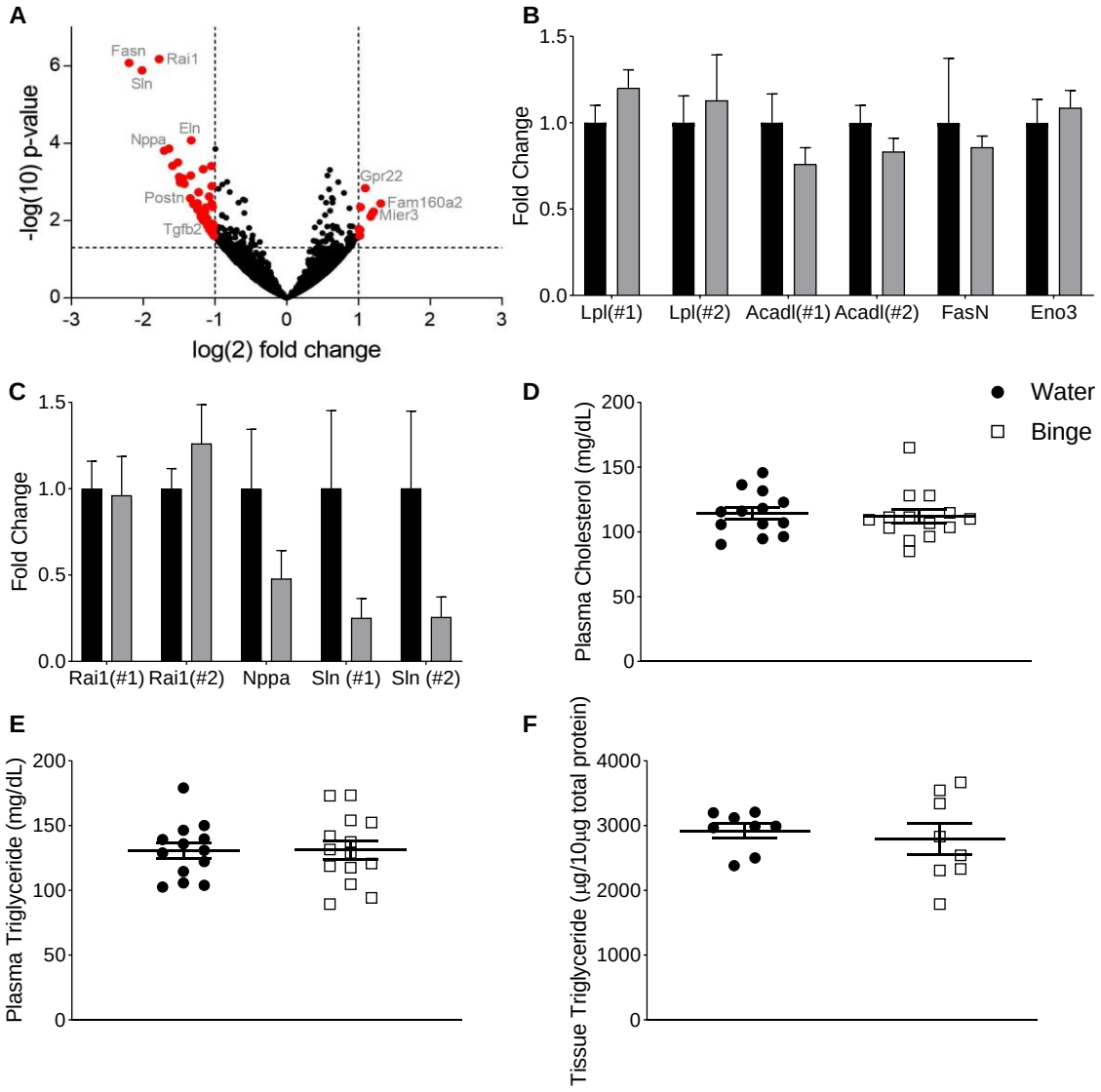

Figure 13. Binge Alcohol Exposure Changed Various Gene Expressions but not yet to Lipid Profile. (A) Volcano plot analysis of RNA seq data on changes in gene expressions by binge alcohol exposure. Expressions of some representative genes for cardiac fatty acid metabolism and sarcomere structures are labeled. (B) A few key regulatory genes in fatty acid metabolism that had shown down-regulation from RNA seq, so confirmatory quantitative rtPCR experiments were performed. (C) Genes that are important for cardiac structures and function (sarcolipin and natriuretic peptide A) were also measured mRNA expression using qPCR to confirm the RNA seq data. Retinoic acid induced 1 is a gene that had found to be regulating circadian rhythms and brain development. However, Rai 1 did not show down regulation as expected from the RNA seq data (Water n=6; Binge n=7). (D, E) Plasma cholesterol and triglyceride level were similar between Water (n=13) and Binge group (n=14). (F) Both groups also had LV tissue triglyceride level (Water n=8; Binge n=8).

CHAPTER FIVE

DISCUSSION

Our current understanding of how binge alcohol consumption affects the heart in adolescence is limited. It is important to determine the consequences of how binge pattern alcohol exposure would impact the growing heart. The goal of this thesis project was originally to determine whether binge alcohol exposure affects the structure and function of the adolescent heart the same way as it does in adults. However, this project is the first to show that binge alcohol exposure increased systolic function in adolescence and might slow heart growth. We think the increased systolic function was due to beta-adrenergic activation, which was then supported by our TnI phosphorylation data. In addition, our data also revealed novel findings that short-term binge alcohol exposure in adolescent rats 1) led to mild diastolic function changes, including smaller E/A ratio and increased passive stiffness, compared with Water controls; 2) altered cardiomocyte morphology (increased concentric hypertrophy at the base and middle of the LV, and increased eccentric hypertrophy at LV apex compared to Water group); and 3) initiation of a possible energy substrate utilization switch from myocardial fatty acid metabolism to less efficient glucose mechanism. This project uncovered a possible significant cardiac health risk associated with underage binge drinking.

Adolescent Binge Alcohol Exposure Rat Model and Cardiovascular Studies

We utilized a well-established male rat model in our studies. Rats have a more rapid adolescence than human, so PND 37-44 is approximately equivalent to human early adolescence. We focused on male rats in this project since the same male model has been studied and used for many brain development studies [1, 60, 61]. Gavaging only once per day at 9-10 AM is when corticosterone levels are the lowest in rats (highest in human due to the opposite circadian rhythm) [64,65]. Low corticosterone level in the morning allows us to minimize the maximum stress that could be caused by alcohol administration. Since euthanasia was performed within one hour after the last gavage, there was high level of blood alcohol circulating in the rat's body. The Acute group we introduced allowed us to compare the acute binge dose alcohol administration would impact to the heart, in order to examine effects from episodic binge pattern alcohol exposure to the growing heart. The binge group had two days of H2O equivalent gavage, due to two reasons: 1) to be more physiological relevant since adolescents do not get access to alcohol all the time; 2) to avoid any possible alcohol addiction by the body.

M-Mode Results on Heart Function Changes of Binge Group Adolescent Rats

Our echo data showed post alcohol treatment the Binge group had smaller systolic parameters, increased ejection fraction (EF), and increased fractional shortening (FS). Instead of decreasing systolic function as in adults [73], binge alcohol exposure in adolescence increased systolic function in our study. One possible reason may be due to the activation by beta-adrenergic signaling, and we did identify an increase in phosphorylation of TnI, an important downstream protein of beta-adrenergic signaling

pathway. Further experiments such as cAMP activity assay can be performed to measure the downstream effects of beta-adrenergic activation in adolescent rat hearts.

The heart and body grow rapidly and concurrently in adolescence [21]. Our interesting results showed that binge alcohol exposure in adolescent rats led to a trend of reduced heart growth. In adult patients, alcohol has been associated with increasing heart weight by causing pathological hypertrophy [56]. However, in our adolescent animal model, binge alcohol exposure did not increase heart mass. We hypothesize there is a much more complicated mechanism that was activated by binge alcohol exposure, which involves both reducing physiological hypertrophy and increasing pathological hypertrophy in the Binge rats. Particularly from the echo data, the Binge group only had half of the diastolic dimension increase compared to the Water group post alcohol treatment, while both groups had the same increase in body mass throughout the protocol. Since adolescence is a rapid growth period for both the body and the heart [21], decreasing the ratio of heart weight to body weight could decrease the ability of heart to pump enough oxygenated blood to the body. It might also increase the work burden of the relatively small heart to maintain the body's metabolic demands. Whether the slowed heart growth gradually returns to normal, if they no longer receive binge alcohol exposure, will need to be further investigated.

Young adults with binge pattern drinking habits have higher blood pressure (BP) than age-matched non-binge drinkers [42], so it would be interesting to see if this is also true in adolescents. We have not yet measured BP for adolescent rats in this project. The tail cuff method of pressure recording would be useful to non-invasively measure the blood pressure. In addition, cardiac output (CO) is calculated by stroke volume (SV) *

heart rate (HR). Since echo measurements were performed when rats were under stable 2% isoflurane anesthesia, the daily resting HR may differ when rats are conscious [74]. Although alcohol has been previously shown to cause HR to increase in adolescents shortly after exposure [20], basal HR seems to be maintained after the intoxication in female rat models [75]. The basal HR changes have not yet been reported on male adolescent rats, and it is known that sex is a biological variable in biomedical studies [76, 77]. Telemetry would be a useful tool to measure HR in our male animal groups.

Echo data also suggested LV wall thickening in our Binge group rats after alcohol treatment. Our Water control group had increased LVPWd with time. Wall thickening indicates cardiac hypertrophy in adolescent rats after binge alcohol exposure. It will be interesting to examine whether the thickened LV in Binge group would normalize or gradually worsen if the animals are allowed to mature into adulthood. Since adolescents are likely to persist in their drinking behavior into adulthood, another experimental group with a second set of 8-day binge alcohol exposure would be added to determine long term binge alcohol effects on heart function and structure (Figure 14).

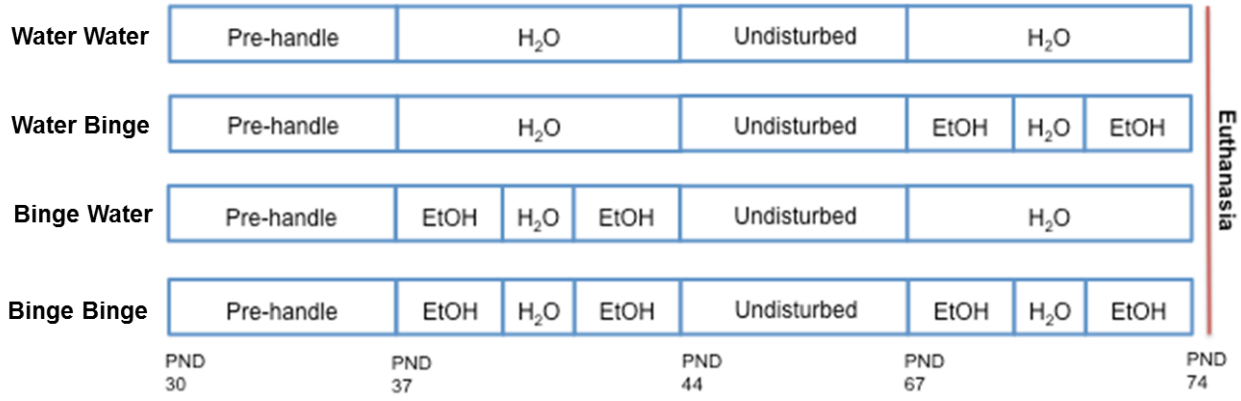

Figure 14. Potential Future Paradigm to Observe the Effects to the Heart for Longer Term when Adolescent Binge Alcohol Exposure Rats Are Allowed to Mature into Adulthood. Water Water: Rats are getting water equivalent throughout the protocol. Water Binge: rats only receive alcohol treatment in adult period. Binge Water: rats stop receiving alcohol after PND 44 and allow to mature into adulthood. Binge Binge: Rats receive first 8 days of binge alcohol exposure in adolescence and another 8 days of binge pattern alcohol exposure in adulthood.

Diastolic Function Alterations after Binge Alcohol Exposure

We were able to identify diastolic dysfunction at the myofilament level by measuring the individual skinned cardiomyocyte passive stiffness. We investigated the spring-like structural protein titin isoform changes by binge alcohol exposure in adolescence and found similar titin isoforms ratio between two groups. Previous research has shown end-stage failing human hearts with dilated cardiomyopathy had isoform transitions to the more compliant N2BA isoform [51, 78], although our experimental Binge group maintained different but normal cardiac function comparing with Water controls. We think this is because our paradigm was only for a short period of exposure and the Binge group was far from being end-stage heart failure. While the paradigm might be relatively short exposure for observing titin isoform switch (t1/2=3.5 days [69]), post-translational modifications (PTM) on titin protein has been found to play a very important role in regulating passive stiffness of the myocyte. One study found that adult heart failure patients tend to have both a titin isoform switch to N2BA and hypophosphorylation on certain regions of the protein [79]. In addition, another study showed that specific hyperphosphorylation on titin spring element PEVK S26 contributed to the passive stiffness in hearts with diastolic dysfunction [80]. Moreover, our TnI phosphorylation data suggested beta-adrenergic signaling activation by binge alcohol exposure in adolescence, and beta-adrenergic activation has shown to alter titin phosphorylation

which decreased passive stiffness [81]. Mass spectrometry would be a useful tool to measure titin PTM changes in adolescent rats after binge alcohol exposure.

Our Doppler data showed smaller E/A ratio in Binge group comparing to Water controls at post treatment. Besides changes in myofilament proteins, remodeling of extracellular matrix (ECM) is another major factor of diastolic stiffness (Figure 11). Myocardial fibrosis by ECM remodeling, which fibroblasts increase collagen stiffer isoform I expression and reduce compliant collagen III expression, is shown to significantly increase passive stiffness and diastolic dysfunction [68, 82]. Alcohol exposure has been found to up regulate many ECM encoded gene expressions in adult rat models [83]. This project has not yet studied the ECM composition after binge alcohol exposure in adolescent rats, so Masson's Trichome staining can be performed using our paraffin embedded heart slices to analyze whether binge alcohol exposure increases fibrosis in the heart.

Binge Alcohol Exposure Effects on Adolescent Cardiac Remodeling

In patients with diastolic heart failure, pathological concentric hypertrophy (increases mass and relative wall thickness) or remodeling (normal mass but increased relative wall thickness) can be observed [31]. Our study is unique because all rats underwent physiological hypertrophy during the protocol (increased LVEDD, LVEDV, and LV wall thickening). Even though both the Water group and the Binge group had LV wall thickening, longitudinal comparison at post treatment showed that the Binge group had significantly larger LVPWd diameters compared to the Water controls. Interestingly, we also observed only half of diastolic dimensions increase compared to the Water controls at post treatment, suggesting smaller heart growth.

Pathologically hypertrophied myocardium usually slows LV relaxation [31]. Slower LV relaxation means reduced early ventricular filling from the atria due to the increased LV diastolic pressure, which in turn increases the proportion of blood left in the LA during atrial contraction. Ultimately pathological hypertrophy leads to a smaller E/A ratio. The smaller E/A ratio from the Doppler results and the increased passive tension from the myofilament measurements support the idea that binge alcohol exposure possibly initiated the pathological hypertrophy in adolescent rats.

This project is the first study to show that binge alcohol exposure in adolescence induces different changes in cardiomyocyte morphology at different locations within the LV (both concentric and eccentric cardiomyocyte hypotrophies). Previously, concentric hypertrophy has been shown in an adult murine model after chronic alcohol consumption [84], but the study did not specify or divide LV positions (base, middle, or apex). We think that adolescent cardiomyocytes at the LV apex lengthened, but cardiomyocytes at the LV middle and base thickened after binge alcohol exposure. However, early adolescent cardiomyocyte morphology is not well studied, so it is not clear whether binge alcohol exposure led to pathological remodeling or slowed the normal physiological remodeling of the LV. A sub control cohort of only the first 7-day prehandling protocol will be included for the future study, and the cardiomyocytes at PND37 will be analyzed and then compared with the cardiomyocytes on PND44 post alcohol treatment. There is a possibility that adolescence binge alcohol exposure increased heart pathological hypertrophy but slowed down the normal physiological hypertrophy.

Binge Alcohol Exposure and Myocardial Fatty Acid Metabolism

Our RNA seq data and qPCR results suggested the initiation of a switch from the preferred fatty acid metabolism to a less efficient glucose metabolism in the heart after binge alcohol exposure in adolescent rats. Multiple fatty acid metabolic genes are shown to be down-regulated, such as lpl and fasn. The gradual switch from fatty acid oxidation to glucose metabolism is one of the common characteristics of heart failure [53]. It would be interesting to examine directly the protein expression, so next step would be to perform mass spectrometry to identify protein levels for those genes in the tissue samples. The RNA seq data showed other regulatory gene down regulations, such as Rai 1, a regulatory protein for circadian rhythm. Our data might explain the binge alcohol consumption induced sleep disorders observed in adolescents [85].

Our data conclude that 8 days of binge alcohol exposure does not yet change LV tissue triglyceride level in adolescent rats. Triglyceride buildup in the heart has been reported in chronic alcoholic cardiomyopathy animal models and adult patients [56, 86]. It would be interesting to further study the threshold at which binge alcohol exposure begins to cause triglyceride buildup in adolescents.

Summary

Binge alcohol consumption is common in adolescence and little to nothing is known about how it would affect the growing heart. The overall effects of binge alcohol exposure on the heart have been under appreciated but the cardiovascular risks can be tremendous to adolescents' health. This project for the first time uncovered the structural and functional changes of the heart after binge alcohol exposure during adolescence. Our data suggests novel findings that binge alcohol exposure negatively impacts normal

cardiac growth (including alterations in cardiomyocyte morphology) and heart compliance. The heart had to compensate for the increase in body demands by increasing systolic function through beta-adrenergic signaling. In addition, this project is the first to find that binge alcohol exposure in adolescence down-regulated 58 genes and up-regulated 10 genes in the left ventricle. Future studies are necessary to determine if the alterations we observed would be maintained throughout adulthood.

REFERENCE LIST

1. Torcaso, A., et al., *Adolescent binge alcohol exposure increases risk assessment behaviors in male Wistar rats after exposure to an acute psychological stressor in adulthood.* Psychoneuroendocrinology, 2017. **76**: p. 154-161.

2. Matyas, C., et al., *Chronic plus binge ethanol feeding induces myocardial oxidative stress, mitochondrial and cardiovascular dysfunction, and steatosis.* American Journal of Physiology - Heart and Circulatory Physiology, 2016. **310**(11): p. 1658-1670.

3. Piano, M.R. and S.A. Phillips, *Alcoholic cardiomyopathy: Pathophysiologic insights.* Cardiovascular toxicology, 2014. **14**(4): p. 291-308.

4. Bing, R.J., *Cardiac metabolism: its contributions to alcoholic heart disease and myocardial failure.* Circulation, 1978. **58**(6): p. 965-970.

5. Milicević, G., et al., *Increase in cardiac contractility during puberty.* Coll Antropol., 2003. **27**(1): p. 335-341.

6. Walsh, S., et al., *Cardiomyocyte cell cycle control and growth estimation in vivo—an analysis based on cardiomyocyte nuclei.* Cardiovascular Research, 2010. **86**(3): p. 365-373.

7. Malandraki-Miller, S., et al., *Changing Metabolism in Differentiating Cardiac Progenitor Cells—Can Stem Cells Become Metabolically Flexible Cardiomyocytes?* Frontiers in Cardiovascular Medicine, 2018. **5**: p. 119.

8. Sorokina, N., et al., *Recruitment of Compensatory Pathways to Sustain Oxidative Flux With Reduced Carnitine Palmitoyltransferase I Activity Characterizes Inefficiency in Energy Metabolism in Hypertrophied Hearts.* Circulation, 2007. **115**(15): p. 2033-2041.

9. Mouton, A.J., et al., *Exposure to chronic alcohol accelerates development of wall stress and eccentric remodeling in rats with volume overload.* Journal of molecular and cellular cardiology, 2016. **97**: p. 15-23.

10. Lymperopoulos, A., G. Rengo, and W.J. Koch, *The Adrenergic Nervous System in Heart Failure: Pathophysiology and Therapy.* Circulation research, 2013. **113**(6): p. 10.1161/CIRCRESAHA.113.300308.

11. Taimor, G., K.D. Schlüter, and H.M. Piper, *Hypertrophy-associated Gene Induction after β -Adrenergic Stimulation in Adult Cardiomyocytes.* Journal of Molecular and Cellular Cardiology, 2001. **33**(3): p. 503-511.

12. Vidal, M., et al., *β-Adrenergic receptor stimulation causes cardiac hypertrophy via a Gβγ/Erk-dependent pathway.* Cardiovascular Research, 2012. **96**(2): p. 255-264.

13. *Substance Abuse and Mental Health Services Administration (SAMHSA). 2015 National Survey on Drug Use and Health (NSDUH).* 2014 and 2015.

14. *Office of Juvenile Justice and Delinquency Prevention. Drinking in America: Myths, Realities, and Prevention Policy*. 2005.

15. Grant, B.F. and D.A. Dawson, *Age at onset of alcohol use and its association with DSM-IV alcohol abuse and dependence: results from the national longitudinal alcohol epidemiologic survey.* Journal of Substance Abuse, 1997. **9**: p. 103-110.

16. McCambridge, J., J. McAlaney, and R. Rowe, *Adult consequences of late adolescent alcohol consumption: a systematic review of cohort studies.* PLoS medicine, 2011. **8**(2): p. e1000413-e1000413.

17. Andreasson, S., P. Allebeck, and A. Romelsjö, *Alcohol and mortality among young men: longitudinal study of Swedish conscripts.* British medical journal (Clinical research ed.), 1988. **296**(6628): p. 1021-1025.

18. Molina, P.E. and S. Nelson, *Binge Drinking's Effects on the Body.* Alcohol research : current reviews, 2018. **39**(1): p. 99-109.

19. DeWit, D.J., et al., *Age at First Alcohol Use: A Risk Factor for the Development of Alcohol Disorders.* American Journal of Psychiatry, 2000. **157**(5): p. 745-750.

20. Crews, F.T., et al., *Binge Ethanol Consumption Causes Differential Brain Damage in Young Adolescent Rats Compared With Adult Rats.* Alcoholism: Clinical and Experimental Research, 2000. **24**(11): p. 1712-1723.

21. Maresh, M.M., *GROWTH OF THE HEART RELATED TO BODILY GROWTH DURING CHILDHOOD AND ADOLESCENCE.* Pediatrics, 1948. **2**(4): p. 382.

22. Naqvi, N., et al., *A proliferative burst during preadolescence establishes the final cardiomyocyte number.* Cell, 2014. **157**(4): p. 795-807.

23. Maillet, M., J.H. van Berlo, and J.D. Molkentin, *Molecular basis of physiological heart growth: fundamental concepts and new players.* Nature reviews. Molecular cell biology, 2013. **14**(1): p. 38-48.

24. Capalbo, D., et al., *Growth Hormone Improves Cardiopulmonary Capacity and Body Composition in Children With Growth Hormone Deficiency.* The Journal of Clinical Endocrinology & Metabolism, 2017. **102**(11): p. 4080-4088.

25. Wang, K.C.W., et al., *Early origins of heart disease: Low birth weight and the role of the insulin-like growth factor system in cardiac hypertrophy.* Clinical and Experimental Pharmacology and Physiology, 2012. **39**(11): p. 958-964.

26. Janz, K.F., J.D. Dawson, and L.T. Mahoney, *Predicting Heart Growth During Puberty: The Muscatine Study.* Pediatrics, 2000. **105**(5): p. e63.

27. de Lucia, C., A. Eguchi, and W.J. Koch, *New Insights in Cardiac β-Adrenergic Signaling During Heart Failure and Aging.* Frontiers in Pharmacology, 2018. **9**: p. 904.

28. Kentish Jonathan, C., et al., *Phosphorylation of Troponin I by Protein Kinase A Accelerates Relaxation and Crossbridge Cycle Kinetics in Mouse Ventricular Muscle.* Circulation Research, 2001. **88**(10): p. 1059-1065.

29. Frank, K.F., et al., *Sarcoplasmic reticulum Ca2+-ATPase modulates cardiac contraction and relaxation.* Cardiovascular Research, 2003. **57**(1): p. 20-27.

30. Myagmar, B.-E., et al., *Adrenergic Receptors in Individual Ventricular Myocytes: The Beta-1 and Alpha-1B Are in All Cells, the Alpha-1A Is in a Subpopulation, and the Beta-2 and Beta-3 Are Mostly Absent.* Circulation research, 2017. **120**(7): p. 1103-1115.

31. Nagueh, S.F., et al., *Recommendations for the Evaluation of Left Ventricular Diastolic Function by Echocardiography.* Journal of the American Society of Echocardiography, 2009. **22**(2): p. 107-133.

32. Nagueh, S.F., et al., *Recommendations for the Evaluation of Left Ventricular Diastolic Function by Echocardiography: An Update from the American Society of Echocardiography and the European Association of Cardiovascular Imaging.* J Am Soc Echocardiogr, 2016. **29**: p. 277-314.

33. Nagueh Sherif, F., et al., *Altered Titin Expression, Myocardial Stiffness, and Left Ventricular Function in Patients With Dilated Cardiomyopathy.* Circulation, 2004. **110**(2): p. 155-162.

34. Medicine, T.T.D.C.C.o.T.J.S.o.U.i., *Standard measurement of cardiac function indexes.* Journal of Medical Ultrasonics, 2006. **33**(2): p. 123-127.

35. Rodrigues, P., et al., *Association Between Alcohol Intake and Cardiac Remodeling.* Journal of the American College of Cardiology, 2018. **72**(13): p. 1452-1462.

36. van Berlo, J.H., M. Maillet, and J.D. Molkentin, *Signaling effectors underlying pathologic growth and remodeling of the heart.* The Journal of clinical investigation, 2013. **123**(1): p. 37-45.

37. Bristow, M.R., et al., *Decreased Catecholamine Sensitivity and β-Adrenergic-Receptor Density in Failing Human Hearts.* New England Journal of Medicine, 1982. **307**(4): p. 205-211.

38. Bristow, M.R., et al., *β1- and β2-adrenergic-receptor subpopulations in nonfailing and failing human ventricular myocardium: Coupling of both receptor subtypes to muscle contraction and selective β1-receptor down-regulation in heart failure.* Circulation Research, 1986. **59**: p. 297-309.

39. Gu, L., et al., *Cardiovascular responses and differential changes in mitogen-activated protein kinases following repeated episodes of binge drinking.* Alcohol and alcoholism (Oxford, Oxfordshire), 2013. **48**(2): p. 131-137.

40. Rimm, E.B., et al., *Moderate alcohol intake and lower risk of coronary heart disease: meta-analysis of effects on lipids and haemostatic factors.* BMJ, 1999. **319**(7224): p. 1523.

41. Seppä, K. and P. Sillanaukee, *Binge Drinking and Ambulatory Blood Pressure.* Hypertension, 1999. **33**(1): p. 79-82.

42. Piano, M.R., et al., *Effects of Repeated Binge Drinking on Blood Pressure Levels and Other Cardiovascular Health Metrics in Young Adults: National Health and Nutrition Examination Survey, 2011 - 2014.* Journal of the American Heart Association, 2018. **7**(13).

43. Kim, S.D., et al., *A Rodent Model of Alcoholic Heart Muscle Disease and Its Evaluation by Echocardiography.* Alcoholism: Clinical and Experimental Research, 2001. **25**(3): p. 457-463.

44. LeWinter, M.M. and H. Granzier, *Cardiac titin: a multifunctional giant.* Circulation, 2010. **121**(19): p. 2137-2145.

45. Linke Wolfgang, A. and N. Hamdani, *Gigantic Business Titin Properties and Function Through Thick and Thin.* Circulation Research, 2014. **114**(6): p. 1052-1068.

46. Bang, M.-L., et al., *The Complete Gene Sequence of Titin, Expression of an Unusual ≈700-kDa Titin Isoform, and Its Interaction With Obscurin Identify a Novel Z-Line to I-Band Linking System.* Circulation Research, 2001. **89**(11): p. 1065-1072.

47. Trombitás, K., et al., *Extensibility of isoforms of cardiac titin: variation in contour length of molecular subsegments provides a basis for cellular passive stiffness diversity.* Biophysical journal, 2000. **79**(6): p. 3226-3234.

48. Trombitás, K., et al., *Cardiac titin isoforms are coexpressed in the half-sarcomere and extend independently.* American Journal of Physiology-Heart and Circulatory Physiology, 2001. **281**(4): p. H1793-H1799.

49. Cazorla, O., et al., *Differential Expression of Cardiac Titin Isoforms and Modulation of Cellular Stiffness.* Circulation Research, 2000. **86**(1): p. 59-67.

50. Wu, Y., et al., *Changes in Titin Isoform Expression in Pacing-Induced Cardiac Failure Give Rise to Increased Passive Muscle Stiffness.* Circulation, 2002. **106**(11): p. 1384-1389.

51. Makarenko, I., et al., *Passive Stiffness Changes Caused by Upregulation of Compliant Titin Isoforms in Human Dilated Cardiomyopathy Hearts.* Circulation Research, 2004. **95**(7): p. 708-716.

52. Lopaschuk, G.D. and J.S. Jaswal, *Energy Metabolic Phenotype of the Cardiomyocyte During Development, Differentiation, and Postnatal Maturation.* Journal of Cardiovascular Pharmacology, 2010. **56**(2).

53. Karwi, Q.G., et al., *Loss of Metabolic Flexibility in the Failing Heart.* Frontiers in cardiovascular medicine, 2018. **5**: p. 68-68.

54. Allard, M.F., et al., *Contribution of oxidative metabolism and glycolysis to ATP production in hypertrophied hearts.* American Journal of Physiology-Heart and Circulatory Physiology, 1994. **267**(2): p. H742-H750.

55. Azevedo, P.S., et al., *Energy Metabolism in Cardiac Remodeling and Heart Failure.* Cardiology in Review, 2013. **21**(3).

56. Hu, C., et al., *Chronic ethanol consumption increases cardiomyocyte fatty acid uptake and decreases ventricular contractile function in C57BL/6J mice.* Journal of molecular and cellular cardiology, 2013. **59**: p. 30-40.

57. Dutta, S. and P. Sengupta, *Men and mice: Relating their ages.* Life Sciences, 2016. **152**: p. 244-248.

58. Sengupta, P., *A Scientific Review of Age Determination for a Laboratory Rat: How old is it in comparison with Human age?* Biomed Int., 2012. **2**: p. 81-9.

59. Sengupta, P., *The Laboratory Rat: Relating Its Age With Human's.* International journal of preventive medicine, 2013. **4**(6): p. 624-630.

60. Asimes, A., et al., *Binge Drinking and Intergenerational Implications: Parental Preconception Alcohol Impacts Offspring Development in Rats.* Journal of the Endocrine Society, 2018. **2**(7): p. 672-686.

61. Przybycien-Szymanska, M.M., Y.S. Rao, and T.R. Pak, *Binge-pattern alcohol exposure during puberty induces sexually dimorphic changes in genes regulating the HPA axis.* American journal of physiology. Endocrinology and metabolism, 2010. **298**(2): p. E320-E328.

62. Vedell, P.T., et al., *Effects on gene expression in rat liver after administration of RXR agonists: UAB30, 4-methyl-UAB30, and Targretin (Bexarotene).* Molecular pharmacology, 2013. **83**(3): p. 698-708.

63. Gao, R.-R., et al., *Traditional Chinese medicine Qiliqiangxin attenuates phenylephrine-induced cardiac hypertrophy via upregulating PPARγ and PGC-1α.* Annals of translational medicine, 2018. **6**(8): p. 153-153.

64. Fulford AJ, H.M., Steckler T, Kalin NH, Reul JMHM, *Handbook of stress and the brain. Part 1: the neurobiology of stress*. 1st ed ed. An introduction to the HPA axis;. 2005, Amsterdam: Elsevier.

65. Qian, X., et al., *A rapid release of corticosteroid-binding globulin from the liver restrains the glucocorticoid hormone response to acute stress.* Endocrinology, 2011. **152**(10): p. 3738-3748.

66. Wood, M.J. and M.H. Picard, *Utility of echocardiography in the evaluation of individuals with cardiomyopathy.* Heart (British Cardiac Society), 2004. **90**(6): p. 707-712.

67. Acquatella, H., L.A. Rodriguez-Salas, and J.R. Gomez-Mancebo, *Doppler Echocardiography in Dilated and Restrictive Cardiomyopathies.* Cardiology Clinics, 1990. **8**(2): p. 349-367.

68. Glenn, T.K., et al., *Role of cardiac myofilament proteins titin and collagen in the pathogenesis of diastolic dysfunction in cirrhotic rats.* Journal of Hepatology, 2011. **55**(6): p. 1249-1255.

69. Isaacs, W.B., et al., *Biosynthesis of titin in cultured skeletal muscle cells.* The Journal of Cell Biology, 1989. **109**(5): p. 2189.

70. Layland, J., R.J. Solaro, and A.M. Shah, *Regulation of cardiac contractile function by troponin I phosphorylation.* Cardiovascular Research, 2005. **66**(1): p. 12-21.

71. Babu, G.J., et al., *Ablation of sarcolipin enhances sarcoplasmic reticulum calcium transport and atrial contractility.* Proceedings of the National Academy of Sciences of the United States of America, 2007. **104**(45): p. 17867-17872.

72. Mullegama, S.V., et al., *RAI1 Overexpression Promotes Altered Circadian Gene Expression and Dyssomnia in Potocki-Lupski Syndrome.* Journal of pediatric genetics, 2017. **6**(3): p. 155-164.

73. Steiner, J.L. and C.H. Lang, *Alcoholic Cardiomyopathy: Disrupted Protein Balance and Impaired Cardiomyocyte Contractility.* Alcoholism, clinical and experimental research, 2017. **41**(8): p. 1392-1401.

74. Brown, H.F., D. Difrancesco, and S.J. Noble, *How does adrenaline accelerate the heart?* Nature, 1979. **280**(5719): p. 235-236.

75. Situmorang, J.H., et al., *Role of neuronal nitric oxide synthase (nNOS) at medulla in tachycardia induced by repeated administration of ethanol in conscious rats.* Journal of biomedical science, 2018. **25**(1): p. 8-8.

76. Beery, A.K. and I. Zucker, *Sex bias in neuroscience and biomedical research.* Neuroscience and biobehavioral reviews, 2011. **35**(3): p. 565-572.

77. Bale, T.L., *Sex matters.* Neuropsychopharmacology, 2019. **44**(1): p. 1-3.

78. Neagoe, C., et al., *Titin Isoform Switch in Ischemic Human Heart Disease.* Circulation, 2002. **106**(11): p. 1333-1341.

79. Gotzmann, M., et al., *Alterations in Titin Properties and Myocardial Fibrosis Correlate With Clinical Phenotypes in Hemodynamic Subgroups of Severe Aortic Stenosis.* JACC: Basic to Translational Science, 2018. **3**(3): p. 335.

80. Hudson, B., et al., *Hyperphosphorylation of Mouse Cardiac Titin Contributes to Transverse Aortic Constriction-Induced Diastolic Dysfunction.* Circulation Research, 2011. **109**(8): p. 858-866.

81. Falcão-Pires, I., et al., *Diabetes Mellitus Worsens Diastolic Left Ventricular Dysfunction in Aortic Stenosis Through Altered Myocardial Structure and Cardiomyocyte Stiffness.* Circulation, 2011. **124**(10): p. 1151-1159.

82. Zile, M.R., et al., *Myocardial Stiffness in Patients with Heart Failure and a Preserved Ejection Fraction: Contributions of Collagen and Titin.* Circulation, 2015. **131**(14): p. 1247-1259.

83. Steiner, J.L., et al., *Alcohol Differentially Alters Extracellular Matrix and Adhesion Molecule Expression in Skeletal Muscle and Heart.* Alcoholism, clinical and experimental research, 2015. **39**(8): p. 1330-1340.

84. Law, B.A., S.P. Levick, and W.E. Carver, *Alterations in Cardiac Structure and Function in a Murine Model of Chronic Alcohol Consumption.* Microscopy and Microanalysis, 2012. **18**(3): p. 453-461.

85. Popovici, I. and M.T. French, *Binge drinking and sleep problems among young adults.* Drug and alcohol dependence, 2013. **132**(1-2): p. 207-215.

86. Tsiplenkova, V.G., A.M. Vikhert, and N.M. Cherpachenko, *Ultrastructural and histochemical observations in human and experimental alcoholic cardiomyopathy.* Journal of the American College of Cardiology, 1986. **8**(1, Supplement 1): p. 22A-32A.

VITA

The author, Lizhuo Ai, was born in Shandong, China on December 27, 1994 to Dr. Hongqi Ai and Yunrong Zhang. She attended the Millsaps College in Jackson, MS where she earned a Bachelor's of Science, cum laude, in Biology with minors in Chemistry and Psychology in May 2016. After graduation, Lizhuo Ai matriculated into the Loyola University Chicago Stritch School Cell and Molecular Physiology Graduate Program. She began her graduate education under the mentorship of Dr. Jonathan Kirk.